ADVANCED SENSOR RESEARCH Open Access
www.advsensorres.com

Single-Molecule Electronic Biosensors: Principles and Applications

Xinyue Chang, Yani Huo, Cong Zhao, Wanqi Sun, Ziqi Song, Ziyuan Qi, Jinying Wang, Chuancheng Jia,* and Xuefeng Guo**

Single-biomolecule electronic sensing techniques are of great importance in many fields, from medical diagnosis to disease surveillance. As the physiological changes of single biomolecules can be converted into measurable electrical signals, single-molecule electronic biosensors can realize real-time, highly sensitive, and high-bandwidth detection of individual intra- or inter-molecular interactions. These powerful single-molecule sensing devices have demonstrated key advantages in precisely providing rare and detailed intermediate information along reaction pathways and revealing unique properties hidden in ensemble measurements. This review summarizes significant advances in single-molecule electronic biosensors, emphasizing biomolecule recognition, interaction, and reaction dynamics at the single-molecule level. Sensor configurations, sensing mechanisms, and representative applications are also discussed. Furthermore, a perspective on the use of photoelectric integrated systems for synchronous sensing of the electrical and optical signals of single biomolecules is provided.

1. Introduction

Due to the rapid advances in materials science and nanotechnology, reliable and sensitive detections of biomolecules have been effectively performed down to the single-molecule level.[1,2] Single-molecule detection techniques offer great details on the information of biological activities hidden in ensemble measurements. The detailed information is capable of accurately providing unique insights into the structural characteristics, conformational changes, and reaction dynamics of biomolecules.[3–5]

Various technologies, such as surface-enhanced Raman spectroscopy,[6] super-resolution fluorescence microscopy,[7] near-field optical microscopy,[8] and single-molecule force spectroscopy,[9] have been developed to achieve single-molecule detection over the past few decades. Among these high-resolution and high-sensitive techniques, single-molecule electronic techniques have several unique properties, including real-time, label-free, and non-destructive detections with high signal bandwidth, long observation time, and simple device configuration. Therefore, these biosensors have been proven to be promising and powerful tools for ultrasensitive biological detection in the in situ monitoring of single-molecule activities.[10] Moreover, single-molecule electronic biosensors have compatible structures and fabrication processes with wafer-scale semiconductor devices, laying a robust foundation for the combination with integrated circuit (IC) processors toward the development of highly integrated and multiplexed biosensor architectures.

To construct ultrasensitive single-molecule electronic biosensors, the sensing materials are required to have good biocompatibility, fast response time, and excellent electrical properties. Low-dimensional materials have an extremely high surface-to-volume ratio, intrinsic electronic transport, and highly sensitive electrostatic regulation properties, so they hold great potential to develop ultra-sensitive electronic biosensors.[11] In this review, we will introduce the prominent approaches of designing and fabricating single-molecule electronic biosensors using different low-dimensional materials as sensing elements, including 1D silicon nanowires (SiNWs), 1D single-walled carbon nanotubes (SWCNTs), 2D nanomaterials (such as graphene and molybdenum disulfide), and molecular bridges. We also systematically review the significant advances of single-molecule electronic biosensors and highlight their important applications in detecting individual biological reaction events, such as protein structural dynamics, deoxyribonucleic acid (DNA) hybridization, and

X. Chang, Y. Huo, C. Zhao, W. Sun, Z. Song, Z. Qi, J. Wang, C. Jia, X. Guo
Center of Single-Molecule Sciences
Institute of Modern Optics
College of Electronic Information and Optical Engineering
Nankai University
38 Tongyan Road, Jinnan District, Tianjin 300350, P. R. China
E-mail: wang4205@purdue.edu; jiacc@nankai.edu.cn; guoxf@pku.edu.cn

J. Wang
Network for Computational Nanotechnology
Purdue University
West Lafayette, IN 47907, USA

X. Guo
Beijing National Laboratory for Molecular Sciences
National Biomedical Imaging Center
College of Chemistry and Molecular Engineering
Peking University
292 Chengfu Road, Haidian District, Beijing 100871, P. R. China

The ORCID identification number(s) for the author(s) of this article can be found under https://doi.org/10.1002/adsr.202200084

DOI: 10.1002/adsr.202200084

antibody-antigen assays. Finally, a prospect of optimization based on single-molecule electrical and optical integrated systems is also discussed.

2. Working Mechanism of Single-Molecule Electronic Biosensors

The simple and reliable detection of individual biomolecular activities is essential to drug discovery, medical diagnosis, and virus detection. A key challenge in the field of modern biosensors is to realize real-time detection of the in situ activities in natural samples at single-molecule resolution.[12] Single-molecule electronic biosensors are capable of label-free and real-time detection of a biological molecule (including proteins, viruses, and nucleic acids) with high sensitivities and high specificity. In this section, we will introduce the working mechanism of single-molecule electronic biosensors and describe the Debye screening effect, which is a key factor affecting the detection performance.

2.1. Principle of Single-Molecule Electronic Sensing

The structure of single-molecule electronic biosensors contains a sensing nanochannel spanning source and drain electrodes in a current monitoring circuit (**Figure 1**a).[13] Their working mechanism is based on quickly detecting the change in the electrical circuit conductance. When biomolecules bind to the channel surface or interact dynamically with each other, the electrical resistance of channel materials will be changed, resulting in observed changes in current, which provides a direct and readable representation of the molecular activities. In this regard, the field-effect biosensor is the most widely used sort of single-molecule electronic biosensors. During the process of operating a single-molecule field-effect biosensor, signal detection is achieved by allowing the target molecular electrostatic potential to electrostatically modulate electron fluxes of the conductive channel.[14] The molecularly gated sensing mechanism can quickly convert the interactions of target molecules into real-time readable electrical signals.

Many efforts have been made to explore the better performance of single-molecule electronic biosensors based on near field sensing, in which the size of sensing channel nanomaterials is of the same scale as most biological entities (such as proteins, nucleic acids, viruses, etc.).[15] Specifically, single-molecule electronic biosensors usually use SiNWs, SWCNTs, 2D materials, or molecules with a specific nanometer or even sub-nanometer size as conductive channels. Their matched size scale ensures that the changes of a captured molecule can directly modulate the carrier density at the small nanometric sensing channel surface. Due to the field effect or scattering effect, once a single biomolecule interacts with the conductive channel, the change of the sensing site will noticeably affect the conductivity of the entire device like a switch valve. This makes the electronic nanobiosensors sensitive enough to detect biomolecules at the single-molecule level. The high-quality channel material surface and the intact electrode-channel contact interface associated with these single-molecule electronic biosensors can also improve the single-molecule sensing sensitivity.[16]

To realize effective single-molecule detection of biomolecules, single biomolecules are usually connected to the surface of conductive nanochannels through covalent or non-covalent approaches. The dynamic behaviors of single molecules can be directly identified and monitored by the electrical signals of the devices. In addition, the tethered single molecule can act as a probe to interact with other target molecules in the solution. This method of probe-target interactions can detect target molecules with single-molecule resolution in a large concentration range (aM–mM). The concentrations of target biomolecules for single-molecule detection with representative electronic biosensors are summarized and listed in **Table 1**.

To better understand the working mechanism of single-molecule electronic biosensors, the monitoring of a molecule (or even an ion) by the field-effect sensor is the basis. For example, a new approach for the direct detection of single hydrogen ion (H^+) capture/emission events at the solid/liquid interface, within a sub-10-nm electrical double layer (EDL) which is the gate of SiNW sensors, was realized.[17] In this study, the detection of a single hydrogen ion was achieved by using an individually activated Si dangling bond (DB) on the surface as the single H^+ receptor via the local Coulomb scattering effect (Figure 1b). The key to detecting a charge is the extremely low intrinsic device noise, which must be lower than the single charge signal. This work reduces the sensor noise by annealing the SiNW structure in the H_2 ambient and optimizing the number of H^+ receptors (i.e., surfacial Si DBs) through a native oxide etching step in buffered hydrogen fluoride. These methods (such as the meticulous processing of sensing channel materials and the fine control of the number of detection sites) are demonstrated to be key for further improvement of the single-molecule electronic biosensor fabrication/performance. In the sensing environment and the circuit, the current signals of electronic biosensors, which are extremely sensitive to the changes of the target analyte, are very weak and limited by the background noise of potential fluctuations. Therefore, it is imperative to improve the signal-to-noise ratio (SNR) level in order to improve the detection ability of single-molecule electronic biosensors and make them more stable and sensitive. The sensitivity of biosensors can be enhanced via adjusting the channel structure, electrode-channel contact resistance, and scattering of recognition sites. Moreover, biosensors should work in the linear sensing scope (the output current is proportional to the input gate voltage). Within this range, the tethered single molecule can precisely gate the source-drain current as shown in I–V_g characteristics (Figure 1c).[18] The direct-current response underlies the sensing performance of electric sensors. Once the analyte is added, the magnitude of current as a function of time changes immediately (Figure 1d). These two-level fluctuations of the current develop the random telegraph noise (RTN) that can work as a reliable predictor of a single target biomolecule binding and unbinding at the sensing site.[19]

2.2. Debye Screening Effect in Single-Molecule Electronic Sensing

Single-molecule electrical detection involves the transduction of molecular properties into electrical signals. However, due to the ionic double layer adsorbed around the surface of the conductive channel, the formed ionic diffusing barrier has a charge

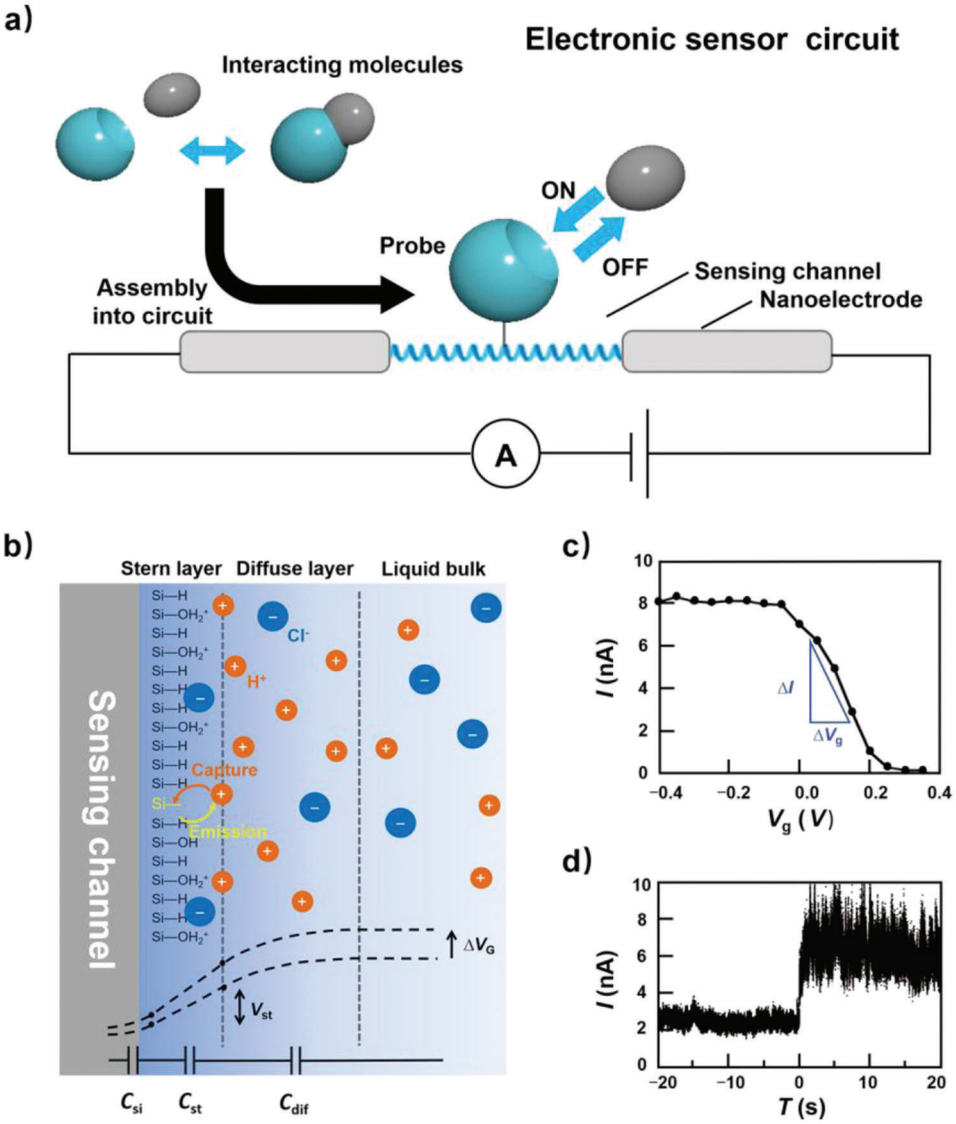

Figure 1. The working mechanism of single-molecule electronic biosensors. a) Schematic of the single-molecule electronic sensing circuit. Reproduced under terms of the CC-BY-NC-ND license.[13] Copyright 2022, The Authors, published by National Academy of Science. b) Schematic of the sensing of a single hydrogen ion. Reproduced under terms of the CC-BY- license.[17] Copyright 2021, The Authors, published by American Association for the Advancement of Science. c) Rapid response of current with electrolytic gating. The inset shows a linear sensing scope where the output current is proportional to the input gate voltage. d) Real-time sensing current with binding a biomolecule. c,d) Reproduced under terms of the CC-BY license.[18] Copyright 2012, The Authors, published by American Association for the Advancement of Science.

screening effect on the target molecules to be detected in ionic solutions. The detection of biomolecules in physiological solutions with the high ionic strength still lags far behind the expected potential of single-molecule electronic biosensors.

Specifically, to create a suitable physiological environment in single-molecule biological measurements based on field-effect sensing, the analyte is typically dissolved in electrolytes, such as phosphate buffer solution. In this solution, the ions with opposite charges to the charged channel (also called counterions) will be attracted and form an EDL in the vicinity of the charged channel surface (**Figure 2**a).[20] Therefore, the EDL will undergo charge screening outside the counterion layer, whose length is called the Debye length (λ_D) and can be defined as follows:[21]

$$\lambda_D = \sqrt{\frac{\epsilon k_B T}{q^2 c}} \quad (1)$$

where ϵ is the dielectric permittivity, c is the ionic strength of the electrolyte, q is the electron charge, T is the absolute temperature, and k_B represents Boltzmann's constant. Thus, although counterions accumulate around the charged channel surface, only the charge changes of biomolecules within the Debye length can significantly cause the change of the source-drain current flow. Meanwhile, the limitations of Debye screening on the channel surface can be quantified. For a point-functionalized carbon nanotube field-effect platform, the amplitude of RTN data (linearity

Table 1. Detection concentrations of single-molecule electronic biosensors.

Sensor type	Probe	Target	Target concentration	Ref.
SiNW	Hairpin DNA	ssDNA	1 μM	[50]
	DNA	DNA-binding protein (WRKY1N)	10 μM	[51]
SWCNT	Taq DNA polymerase	dNTP	10 μM	[63]
	ssDNA	Complementary ssDNA	1–100 nM	[64]
	ssDNA	Complementary ssDNA	100 nM–1 μM	[3]
	DNA polymerase I (Klenow fragment)	dNTP or ddNTP	10 μM	[60]
		Native dNTP	10 μM	[61]
		Analog dNTP	100 μM	
Molecular bridge	ssDNA	Complementary ssDNA	10–1000 nM	[13]
	DNA	DNA polymerase	0.008–3.8 μM	
	DNA polymerase	DNA	2.5–15 μM	
	DNA aptamer	SARS-CoV-2 S protein	0.1–1000 nM	
	ssDNA	Antifluorescein antibody	0.5–3.5 μM	
	CRISPR/Cas enzyme	dsDNA	0.1–100 pM	
	DNA	Ethidium bromide	0.5 pM	[99]
		SYBR Green I	0.02 pM	
	ssDNA	mRNA	>20 aM	[96]
	G4 aptamer	α-thrombin	2.6 aM–260 nM	[105]
	Biotin	Streptavidin	0.2 ng mL^{-1}	[107]
	Φ29 polymerase	dNTP	1 mM	[113]

with normalized resistance change) in the conductance changes synchronously with the Debye length (Figure 2b).[22] Therefore, the decrease in Debye length can be reflected by the fluctuations of RTN.

For typical biosample solutions at room temperature, the Debye length is ≈0.7–2.2 nm, so the electrical detection of biomolecules needs to operate under low ionic strength conditions of about 10 mM. Unfortunately, the physiologically ionic strength of most complex biosamples is above 100 mM. Thus, finding approaches to overcome Debye screening is of critical importance. In the past decades, several strategies have been reported to overcome the ionic screening effects, for example, improving channel materials morphology, modulating devices using electrical fields, and designing the decoration of biomolecules.[23] Investigations into the decoration of special aptamers are an important example of overcoming Debye length limitations of biomolecule sensing.[24–26] Specifically, binding deoxyribonucleotide aptamers on the surface of the channel material (nanometer-thin In_2O_3) can realize highly sensitive detection of small molecules under physiological high-ionic strength conditions.[27] The stem-loop negatively charged DNA will change its conformation after target binding. When the substantial portions of the DNA aptamer backbones move closer to the surface of n-type In_2O_3 channels (Figure 2c), the electric field distribution on the channel material surface will change, increasing the electrostatic repulsion to charge carriers and decreasing the transconductance of the field-effect sensor. On the contrary, when the aptamer moves away after capturing the target, (Figure 2d) superficial carrier concentration and transconductance will increase. In addition, passivating the channel surface by decorating the porous and biomolecule permeable polymer layer is also used to overcome the ionic screening effects. A typical example is the SiNW-based field-effect sensor with polyethylene glycol (PEG) modification. The field-effect sensor shows the direct and sensitive detection of a prostate-specific antigen in physiological solutions of high ionic strength up to 150 mM (Figure 2e).[28] The polymer layer of PEG can effectively change the dielectric properties in the local ionic environment, further overcoming the Debye screening and enabling real-time detection of biomolecules in physiologically ionic strength solutions (Figure 2f). Despite these efforts to overcome the limitation of Debye screening, these near-field electronic biosensors still face considerable technical challenges in the further practical application of single-molecule detection in situ physiological environments.

3. Silicon Nanowire-Based Single-Molecule Biosensors

Semiconducting nanowires provide new opportunities for the detection of single molecules due to their large surface-to-volume ratio, excellent electrical properties, fast signal response, and natural matching with the size of biomolecules.[29] SiNWs are widely used to construct single-molecule electronic biosensors due to their unique advantages such as adjustable electrical properties, controllable diameter, rich surface chemical groups, and framework compatibility with common semiconductor processes and quantum devices. SiNW-based single-molecule biosensors can realize ultra-sensitive and label-free biological detection in many fields, such as clinical diagnostics, biomedical research,[10] and drug development.[30] Here, we mainly introduce the

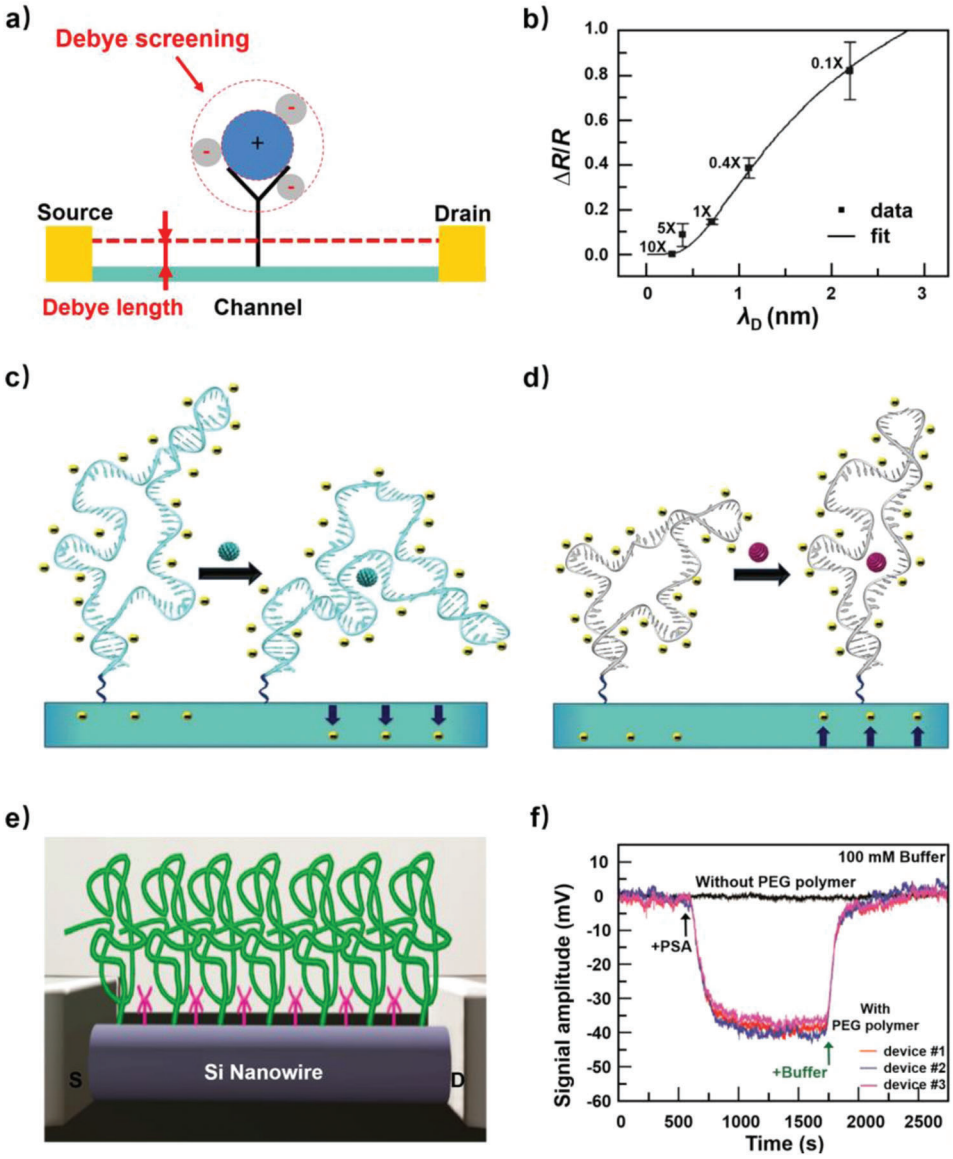

Figure 2. Debye screening effect in biomolecular sensing. a) Schematic of the charge screening effect of a single-molecule biosensor. Reproduced with permission.[20] Copyright 2016, WILEY-VCH. b) Normalized resistance changes versus buffer concentration, where the increasing buffer concentration reduces the Debye length along with the decrease of normalized resistance change. Reproduced with permission.[22] Copyright 2011, American Chemical Society. c) Schematic of the stem-loop aptamer reorientations closer to the channel surface upon target binding. d) Schematic of the stem-loop aptamer reorientations away from the channel surface upon target capture. c,d) Reproduced with permission.[27] Copyright 2018,American Association for the Advancement of Science. e) Polymer (green) surface modification to overcome Debye screening. f) Real-time signal amplitude of sensing current following the modification with the PEG layer. e,f) Reproduced with permission.[28] Copyright 2015, American Chemical Society.

fabrication methods of SiNW-based devices, the strategies to improve the sensitivity and achieve single-molecule detection, and the dynamic detection of single biomolecules, which lay a certain foundation for its application in a wide range of different fields.

3.1. Fabrication of Silicon Nanowire-Based Devices

In general, there are two major approaches for SiNW synthesis: one is bottom-up growth, represented by chemical vapor deposition (CVD),[31] and the other one is top-down fabrication. Bottom-up growth is an additive technique by which the final morphologies of materials such as SiNWs, films, or quantum dots are progressively self-assembled from molecules or atoms. The top-down method is a subtractive technique, starting with a bulk material and gradually peeling off parts of the material to obtain the desired shape.

To fabricate SiNW-based devices with the bottom-up approach, CVD is the most versatile and simplest method, which can obtain semiconductors with tailored dimensions at the nanoscale. The synthesis of SiNWs via this method can preliminarily realize diameters <20 nm and lengths >1 μm. The small-diameter

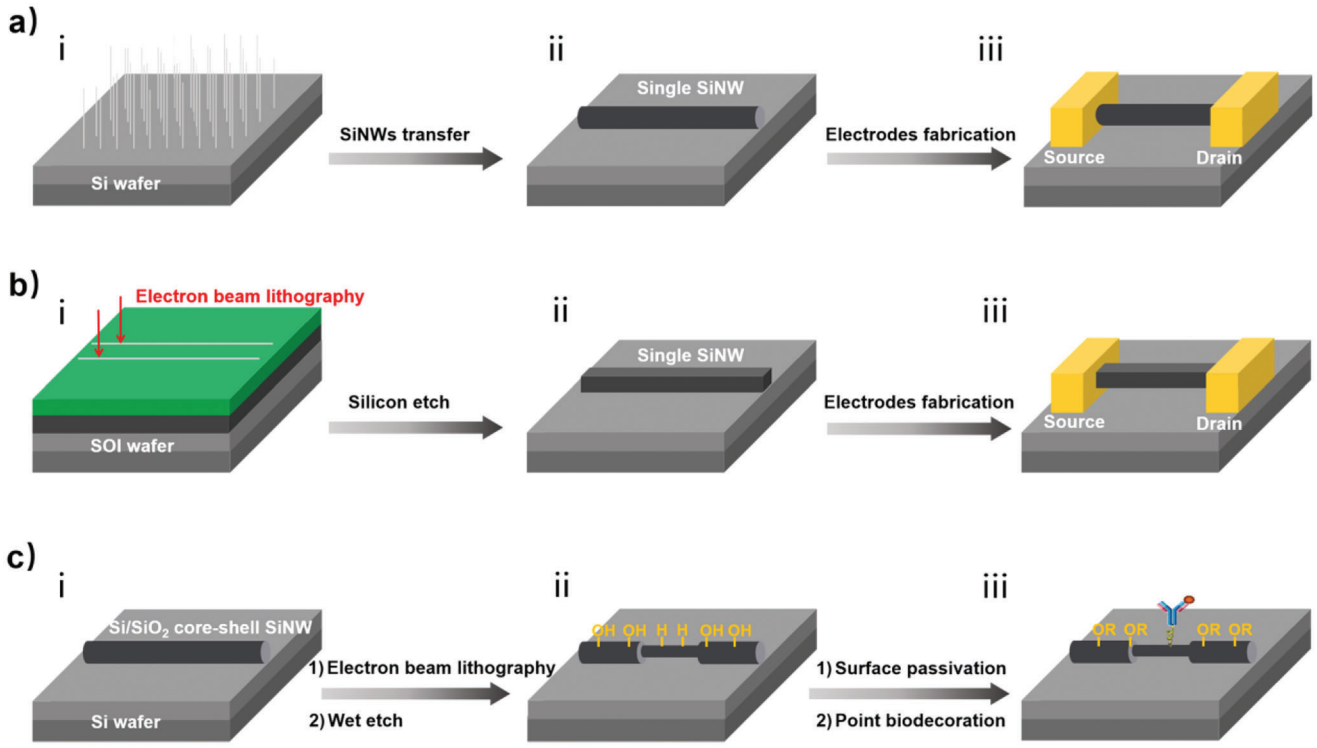

Figure 3. Fabrication of SiNWs. a) Schematic of direct mechano-sliding transfer of CVD-grown SiNWs and fabrication of SiNW-FET devices. Reproduced with permission.[31] Copyright 2022, The Royal Society of Chemistry. b) Top-down nanofabrication process steps of SiNWs. Reproduced under termos of the CC-BY license.[34] Copyright 2016, The Authors, published by PLOS ONE. c) A three-step process used for fabricating SiNW-based single-molecule electronic biosensors. Reproduced with permission.[33] Copyright 2014, Wiley-VCH.

SiNWs are desirable for high-performance electronic devices at the nanoscale.[32] Metal-assisted chemical etching (MACE) is another novel way to obtain SiNWs. This chemical technology can etch micro/nano size features with a high aspect ratio on the silicon substrate, and manufacture nanostructures of various shapes, such as nanopore membranes, nanowires, trenches, 3D objects, and through-holes. The main advantages of the MACE method are its fine control over the structural properties and the realization of vertically aligned SiNWs. In addition, high-quality p-type SiNWs with desired core-shell structure can be uniformed by an Au-catalyzed vapor–liquid–solid (VLS) method.[33] Although VLS has been widely used, there are still some aspects that need to be improved, such as high process temperature, poor structure control, and uneven doping, which limit the integration of SiNWs in devices.

After the successful preparation of the SiNW array, it is necessary to transfer nanowires to further fabricate the device. By controlling the dispersion of nanowires through the transfer process, device fabrication can be better realized. Various transfer methods such as Langmuir-Blodgett film, bubble blowing method, and electric/magnetic field induced alignment method, etc., have been developed. For instance, a direct mechano-sliding transfer (DMST) of CVD-grown SiNWs has been reported, which greatly simplifies the transfer operation in a solvent-free, fluid-free, and lubrication-free manner (**Figure 3**a).[31] This process is based on the direct physical interaction between nanowire and substrate without any auxiliary means. Through applying an appropriate pressure to the substrate, the transmission of the distribution density of nanowires can be controlled, and the reuse of CVD-grown SiNWs can be realized to improve the efficiency of device fabrication. The experimental results show that the SiNW-FET (field effect transistor) manufactured by the DMST technology not only retains its high quality, but also has excellent surface charge response characteristics and surface modification versatility, which is expected to be applied to academic research and lays a foundation for further exploring the physical properties of new 1D nanomaterials.

In comparison with the bottom-up method, the top-down fabrication method can be processed directly on a silicon wafer, which has good reproducibility and stability. Conventional techniques of top-down etching are based on lithographical methods including photolithography, electron beam lithography, ion beam lithography, and so on. A top-down nanofabrication approach has been used to develop SiNWs from silicon on insulator wafers, including direct-write electron beam lithography, inductively coupled plasma-reactive ion etching, and size reduction processes (Figure 3b).[34] This device can be used for efficient label-free, direct, and higher-accuracy DNA molecular detection. Moreover, the top-down prepared SiNW-FET is fully compatible with the complementary metal oxide semiconductor (CMOS) technology. For instance, the fabrication technology of highly controllable wafer-level SiNW-FET arrays on silicon-on-insulator wafers has been proposed. The design and fabrication of 3000 SiNW-FET array devices on 4-inch wafers with a fine variation rate of over 90% have been realized.[35] The SiNW size deviation of each array is less than ±20 nm. The structure of the top-gate electrode

is redesigned to protect the SiNWs when exposed to the external environment. The entire fabrication process of the SiNW array is compatible with the CMOS technology, using traditional microfabrication technology, such as lithography, wet etching, and reactive ion etching. These arrays show excellent electrical properties and highly sensitive determination of pH and nitrogen dioxide, laying the foundation for large-scale applications of SiNWs. In addition, the detection of circulating tumor DNA in human serum samples was successfully achieved by silanization of DNA probes with uniform size and high response SiNW-FET arrays mentioned above.[36]

3.2. Strategies for Improving the Sensitivity of Silicon Nanowire-Based Devices

The high sensitivity of SiNW-based devices is needed to realize single-molecule biosensing. The basic parameters such as doping concentration, wire size, and Debye screening length are strongly related to the sensitivity of the monocrystal SiNW-FET. Doping can affect the transfer characteristics of the FET devices. By introducing impurity atoms, the density of free carriers in SiNWs can be controlled and the electrical properties of SiNWs can be adjusted. Lightly or moderately doped SiNWs have been demonstrated to enhance the limit of detection to the attomolar-femtomolar level.[37] For instance, low-doped SiNWs (10^{17} atom cm^{-3}) can increase the detection sensitivity of the device by threefold in comparison with high-doped (10^{19} atom cm^{-3}) devices.[38] The reason for this phenomenon may be that the shielding effect of mobile charge carriers on charge is weakened in nanowires with low doping concentrations.[39]

The main methods to control doping are conventional doping and surface doping.[40] The main conventional dopants are boron and phosphorus, which are used to form p-type and n-type materials, respectively. It can effectively change the conductivities of nanowires on multiple orders of magnitude. Impurity atoms can be introduced into the crystal lattice in the SiNW core by an in situ process, ion implantation, and other related methods.[41] For example, SiNWs fabricated by MACE can be additionally doped using the standard microelectronic thermal-diffusion approach. Phosphorus thermal diffusion doping can be used to control the free charge carrier concentration in SiNWs detected by Raman spectroscopy.[42] In addition, the electric field can also regulate the distribution of dopant atoms.

A general understanding of semiconductor doping is that doping atoms can not only increase the carrier density, but also reduce the carrier mobility, because the ionized doping atoms act as random scattering centers, resulting in carrier localization. From the perspective of conventional doping, the higher the doping concentration in the nanowire is, the lower the carrier mobility will be. Therefore, new surface doping methods have emerged, such as surface passivation doping and surface shell doping. Surface passivation doping built on the known surface transfer doping has been presented. This surface effect allows efficient doping of SiNWs by electron transfer through the surface layer, which provides a large carrier concentration in SiNWs with surface passivation such as hydrogen. The previous study has shown that phosphorus passivation on the SiNW surface can increase the charge transfer and enhance the doping effect.[41] Surface passivation is a promising method for regulating the electrical conductivity of SiNWs. The conventional doped atoms are uniformly distributed in the nanowires, while the shell doping restricts the doping atoms to the shell region of the nanowires in space. Shell doping of a nanowire at a large doping concentration can enhance carrier mobility because of the existence of quasi-mobility edges separating the stable central states with large localization lengths from the strongly localized tail states.

3.3. Strategies for Achieving Single-Molecule Detection of Silicon Nanowire-Based Devices

To meet the requirements of SiNW-based biosensors for single-molecule detection in practical applications, two single-molecule detection methods are proposed: one is to modify the SiNWs at specific sites to detect single molecules; the other is to confine the transmission of the single molecule through nanopore near nanowire.

By etching SiNWs to generate a nanogap, and then modifying the nanogap by surface passivation and point biological decoration, the single-molecule binding sites can be successfully established to achieve single-biomolecule detection (Figure 3c). Specifically, although molecules can be adsorbed on the surface of SiNWs through van der Waals forces, hydrogen bonds, hydrophobic interaction, and so on,[30] this might not be the optimal strategy, because the long-term stability will be affected by environmental changes such as pH, ionic strength, temperature, etc. Usually, the surface of the nanowire is covalently modified to form a firm bond between the biological receptor and the nanowire, which is more conducive to the realization of single molecule detection. A thin silicon oxide layer grows on the surface of SiNWs and acts as an active interface to produce various functional groups (amine, thiol, or aldehyde). Silane chemistry has been widely used for the surface functionalization of nanowires. For instance, 8-hydroxypyrene-1,3,6-trisulfonyl chloride can be immobilized on the surface of SiNWs, which exhibits a pH-dependent adsorption shift. This device can be excited and deprotonated upon illumination at 405 nm, resulting in a current change that depends on pH and the protonation state of molecules.[43] Furthermore, the thin film of SiO_2 can be eliminated via diluted hydrofluoric acid etching to enhance the performance of the SiNW-FET device, followed by the formation of Si-C bonds on the hydrogen termination with olefin derivatives through UV-assisted photochemical hydrosilylation.[29] Photochemical hydrosilylation is a classical method for surface functionalization. A rational bioassay design has been proposed that integrates single-point scattering sites into the circuit.[33] Real-time, label-free detection of influenza (H1N1) virus with single-molecule sensitivity and high selectivity has been realized by using SiNWs as local reporters, in combination with the microfluidic technology. In this work, the crystalline silicon core of SiNWs was exposed to remove the amorphous SiO_2 sheath by applying high-resolution electron beam lithography and wet etching techniques. This process forms nanoscale hydrogen-terminated silicon trenches with dimensions comparable to antibodies, which are essential for single-molecule detection. Photochemical hydrosilylation is confined to the nanogap region and generates the Si-C bonds on the substrate surface. A single H1N1 antibody is

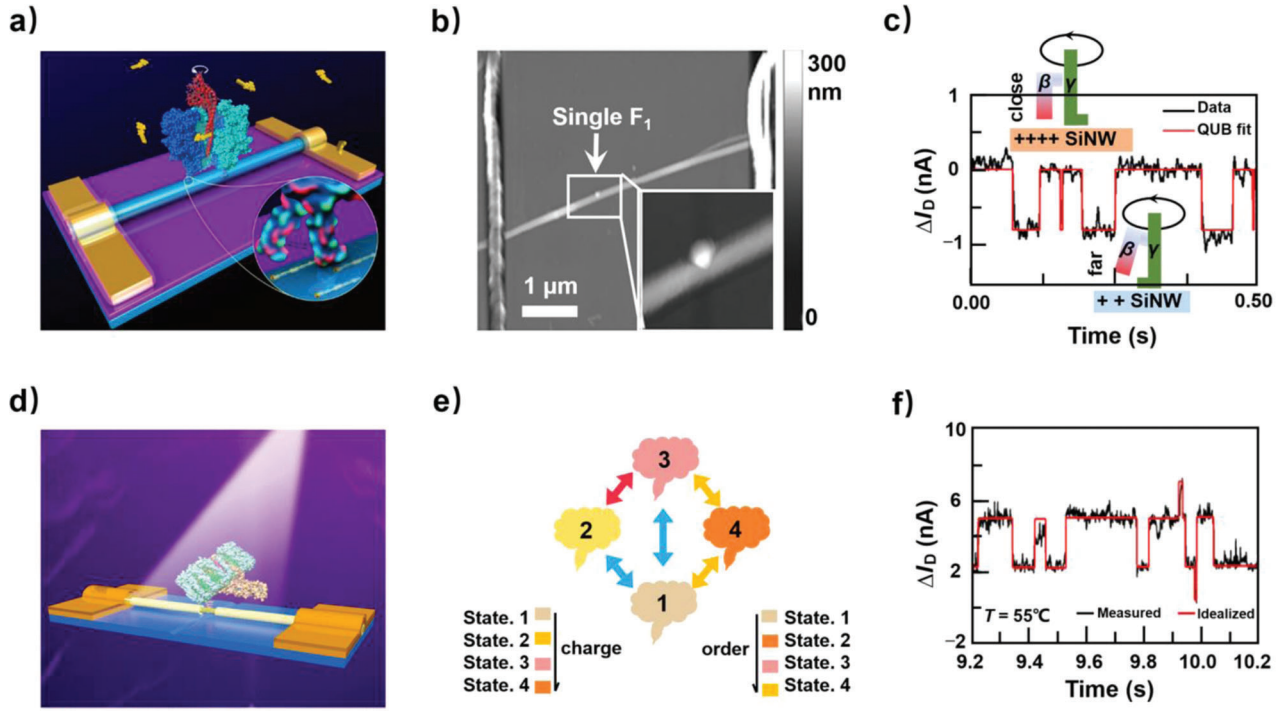

Figure 4. Single protein detection based on SiNW-based sensors. a) Schematic representation of a single F1-modified SiNW FET nanocircuit. b) AFM image showing the success of immobilizing a single F1 on the SiNW surface. c) High and low current states during the hydrolysis of F1. a–c) Reproduced with permission.[46] Copyright 2017, American Chemical Society. d) Schematic diagram of a single-LH1-RC-decorated SiNW-based biosensor. e) The structure of the LH1-RC complex switches between four conformations. f) The immobilization of the LH1-RC complex displays distinct four-level current oscillations. d–f) Reproduced with permission.[41] Copyright 2021, American Chemical Society.

successfully integrated into the circuit by aldehyde groups that could combine with proteins. Direct, rapid, reversible electrical detection of the H1N1 virus has been realized by the combination of antibody-modified SiNW-FET and microfluidic technologies.

Another way to achieve single-molecule detection is to use nanopores to restrict the passage of molecules near nanowires. Specifically, confining a solid nanopore to a nanowire enables not only the detection of molecules by nanopores, but also by nanowire-assisted detection, which has greater advantages over pure nanopore detection, such as faster translocation of direct DNA sequencing. The integrated nanowire–nanopore FET is a novel sensor in which detection is self-aligned and localized at the nanopores,[44] promising high-bandwidth detection to match the problem of fast DNA translocation rates. A key advantage of the nanowire-nanopore FET sensor is the potential for integration and multiplexing within a single analysis chamber without complex microfluidic systems. Compared to direct ion current and other sensor-based detection schemes, this nanowire-nanopore FET sensor offers larger measurement signals, high signal bandwidth, and attractive nanopore size scaling, as well as straightforward integration and multiplexing.

3.4. Single-Biomolecule Detections Based on Silicon Nanowire-Based Sensors

As a suitable single-molecule electrobiological detection platform, a SiNW-FET has the advantages of label-free property and high sensitivity to a single event and can detect the molecular mechanisms of a variety of dynamic biological systems under realistic physiological conditions, such as protein folding, DNA mutation, enzyme activity, etc., which has the significant application value.

SiNWs have been demonstrated as great candidates for the identification of a wide range of biochemical species with high sensitivity and high specificity, especially for the detection of proteins at the single-molecule level. Integrated SiNW-based devices can be used for the detection of lung cancer biomarkers microRNA-126 and carcinoembryonic antigen with high sensitivity and specificity.[45] F1-ATPase (F1) is a bidirectional molecular motor that is essential for cellular physiological processes. F1 hydrolyzes nearly all adenosine-triphosphate (ATP) to fuel the cellular process. To better understand the conformational dynamics of the intrinsic kinetic behavior of ATP hydrolysis, a single-molecule electrical detection approach has been demonstrated, which enables label-free and real-time electrical monitoring of the dynamic process of F1 hydrolysis at the single-molecule/single-event level by using an ultrasensitive SiNW-FET nanocircuit (**Figure 4**a).[46] As shown in Figure 4b, immobilizing a single F1 on the SiNW surface was realized. Reproducible large amplitude two-level current fluctuations can be observed (Figure 4c), where the high current state corresponds to the ATP-binding dwell and the low current state comes from two catalytic dwell of ATP hydrolysis and phosphate groups release. In the latest study, a label-free and real-time measurement method utilizing SiNW-based single-molecule electrical circuits has been

presented that can directly monitor conformational changes of a photosynthetic LH1-RC complex (Figure 4d) that is the core complex of a thermophilic chromosome-lacking filamentous anoxygenic phototroph containing the type II pheophytin-quinone RC and light-harvesting antenna complex.[21] The function of a protein depends on its structural flexibility and conformational change. The structure of the LH1-RC complex vibrates among four conformations with a strong temperature dependence (Figure 4e). As shown in Figure 4f, *I*–*t* measurements fitted well with idealized data, and distinct four-level current oscillations were displayed. At the optimum temperature, states 2 and 3 occupy the dominant conformation of the LH1-RC complex, exhibiting the light-driven jitter of the pigment, which slightly affects the charge distribution of the protein. The conformational variation mainly occurs as harmonic vibration modes, which is beneficial for photon acquisition and heat transmission.

In the field of nucleic acid sensing, a single-strand DNA molecule is immobilized on the surface of SiNWs as the probe/receptor for the detection of its complementary strand. The increase of negative charge on the gate surface translates into an electrical signal that can be used as evidence for nucleic acid hybridization. Neutralizing chimeric DNA probes are used to avoid the interference of background charges from the binding reaction and binding buffer in FET measurements to improve the sensitivity of DNA detection.[47] Under the optimal operating conditions of SiNW-FETs, the neutralized chimeric DNA probe can successfully distinguish single nucleotide polymorphisms in target sequences rich in G-C base pairs.[48]

By using an electronic circuit based on point-modified SiNWs as an electrical probe, the folding/unfolding process of individual hairpin DNAs with single-base resolution and high bandwidth has been directly recorded, which shows a strong temperature dependence on the two-level current oscillations, revealing the thermodynamic and kinetic properties of hairpin DNA hybridization.[49] Continuous, stepwise increases and decreases in device conductance at low temperatures are successfully observed at microsecond timescales, demonstrating the kinetic zipper model of DNA hybridization/dehybridization at the single-base pair level. Based on this study, a straightforward and reliable single-molecule approach has been demonstrated for precise single nucleotide polymorphisms authentication by directly measuring the fluctuations of electrical signals in the electronic circuit that is fabricated by using a high-gain field-effect SiNWs modified with single hairpin DNA (**Figure 5**a).[50] As shown in Figure 5b, the molecular beacon interacted with the target DNA in the solution. When the hairpin DNA attached to the device was exposed to a solution containing complementary target DNA, it was found that the time-averaged current changes $\Delta I_D(t)$ showed a third-order fluctuation behavior (Figure 5c). Allele-specific and accurate single nucleotide polymorphism detection is achieved throughout the process by simply comparing differences in probe-target biostructures.

DNA-protein interaction plays a crucial role in the storage, expression, and regulation of gene information. Compared with ensemble experiments, single-molecule techniques make it possible to investigate individual DNA-protein interactions and provide much more detailed information on transient states, heterogeneous behaviors, and rare events. Recently, the label-free detection of the whole DNA-binding protein (DBP)-DNA interaction process based on high-gain SiNW-FETs by a single molecule electrical monitoring technology has been realized (Figure 5d).[51] WRKY family proteins are important transcriptional factors. The entire process of binding the WRKY domain to DNA has been visualized with high sensitivity and single-base resolution (Figure 5f). The swinging of hydrogen bonds between amino acid residues and bases in DNA induces the dynamic collective motion of DBP-DNA. As shown in Figure 5e, conjugating a Cy3 (a fluorescent reagent) labeled DNA to the SiNW surface enabled the SiNW-FET to be further characterized by stochastic optical reconstruction microscopy (STORM). A single fluorescent spot on the SiNW explicitly guarantees that a single DNA molecule is confined to the surface of the SiNW. It can be predicted that this ultra-sensitive detection platform can be applied to a variety of label-free chemical assays/bioassays at the single-molecule or single-event level, and in further combination with current microelectronics technology, holds great promise for the development of low-noise multiplex detection electronics for precise molecular and even point-of-care clinical diagnosis.

4. Single-Walled Carbon Nanotube-Based Single-Molecule Biosensors

As one of the most popular 1D nanomaterials, SWCNTs have been considered a powerful signal-transducing element to build highly sensitive electronic sensing devices.[18,22] Especially, SWCNT-based sensors have made remarkable progress and showed key advantages, such as excellent biocompatibility, chemical stability, and extremely high carrier mobility.[52] In the following section, the preparation, device construction, and significant applications of SWCNT-based single-molecule biosensors will be introduced.

4.1. Fabrication of Single-Molecule Single-Walled Carbon Nanotube-Based Devices

SWCNTs can be regarded as seamless cylindrical tubular structures formed by rolling a ribbon of graphene along a chiral vector. Due to the unique quasi-1D sp^2 structure and high surface-to-volume ratios, SWCNTs are extremely sensitive to the charge environment of target molecules. SWCNTs can be classified into metallic (m-) and semiconducting (s-) SWCNTs according to their different conductivity.[53] Generally, the zero-bandgap m-SWCNTs are suited for electronic circuits as nanoscale conductors. In contrast, s-SWCNTs with diameter-depended direct bandgap (0.5–1.2 eV) and extremely high carrier mobility up to 10^5 cm^2 $(V{\cdot}s)^{-1}$ are widely used in channel materials of sensors and transistors.[54] For realistic technology applications, commercialized SWCNTs are a mixture of different electrical properties (consisting of m-SWCNTs and s-SWCNTs), which depend on their chirality and diameter. The mixing of carbon nanotubes will seriously damage the performance of electrical components, especially the existence of m-SWCNTs may cause short circuits of field-effect transistors.

Large-scale accurate fabrication of SWCNTs with specific chirality, diameter, and orientation is still challenging.[55] Nowadays, the synthesis methods of carbon nanotubes mainly include arc

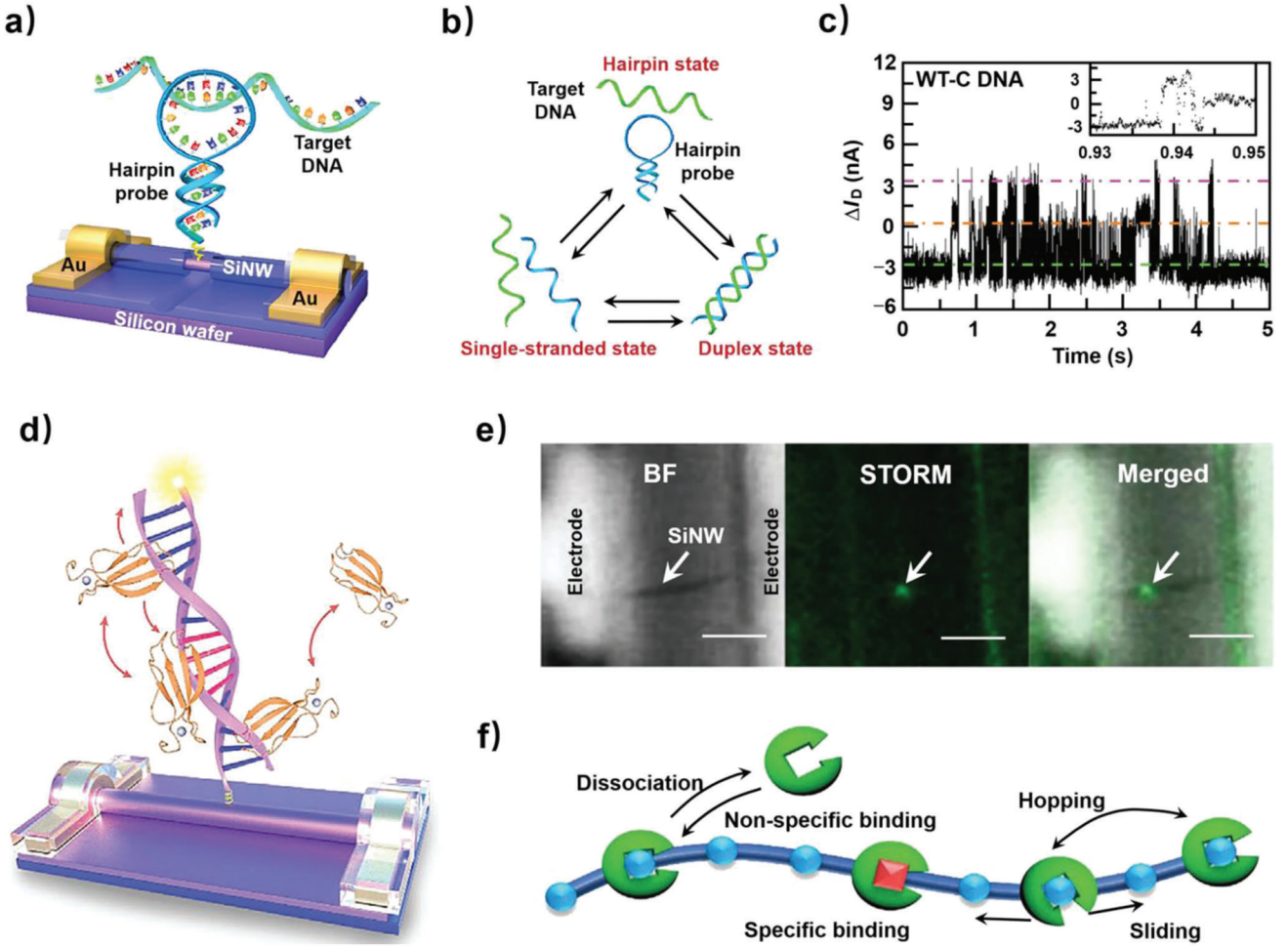

Figure 5. Single biomolecular interactions on SiNW-based sensors. a) Schematic diagram of hairpin probe modified single-molecule biosensor. b) Schematic demonstration of three-phase transitions during hairpin DNA hybridization with the complementary target. c) Source-drain current fluctuations of a single hairpin DNA-decorated SiNW biosensor. a–c) Reproduced under terms of the CC-BY license.[50] Copyright 2017, The Authors, published by Wiley-VCH. d) Schematic of a single-DNA modified SiNW-FET. e) Bright field image (left), STORM image (medium), and the merged image (right) of single-DNA modified device. f) Schematic of the interaction between WRKY1N protein and W-box DNA. d–f) Reproduced under terms of the CC-BY license.[51] Copyright 2021, The Authors, published by Wiley-VCH.

discharge, laser ablation, and catalyst-assisted CVD.[56] Among these methods, CVD is the most popular approach for preparing high-quality SWCNTs with minimal defects. In the synthesis process, to control the chirality of SWCNTs, it is important to select suitable high melting-point catalysts (e.g. iron, nickel, or cobalt nanoparticles) as the template for the nucleation of SWCNTs. Note that before dispersing the catalyst onto the growth substrate, the catalysts need to be diluted to an appropriate concentration for the desired SWCNT density.[57] However, the CVD synthesis methods result in a mixture of m-SWCNTs and s-SWCNTs with varying dimensions. The stochastic nature of the SWCNTs' chirality and diameter will challenge the subsequent fabrication of high-performance devices, so further operations of isolation and purification after growth is necessary. To prepare single-molecule field-effect sensors, electrodes patterned by photolithography are required to contact one SWCNT on average.

For SWCNT grown by the CVD method, in most sensing applications, their surfaces are perfect lattices without suspended bonds, and the probe molecules may be difficult to adsorb on the SWCNT's surfaces. To improve the detection sensitivity and sensing stability, it is essential to functionalize the SWCNT interface with stable biorecognition elements to assist in the connection of probe molecules to channel surfaces. Specifically, the strategy of covalent functionalization involves the partial formation of a localized defect using physical/chemical methods and the introduction of an oxygenated group such as carboxylic acid fragments or carboxyl groups in the SWCNT lattice.[22,58,59] The group on the defect site can be used to attach a certain probe molecule. The covalent functionalization of SWCNTs provides good stability for the detection of biomolecular connections, but the damage to the structure and the disruption of carbon sp^2 bonds will increase the charge scattering, resulting in poor electrical sensing sensitivity and low SNR. In contrast, the non-covalent functionalization maintaining the initial properties of SWCNTs is an attractive alternative.[18,60,61] By using the property of delocalized π bonds in SWCNTs, the non-covalent conjugation can be formed by

π–π stacking to connect probe molecules to the SWCNT channel. Notably, to avoid ensemble averaging of electrical signal recording from multiple molecules of interest, both of the above two functionalization methods require prior coating with passivating layers (Al_2O_3 or poly(methyl methacrylate)) to passivate and protect the SWCNT surface and SWCNT-metal interfaces from the environment. Then, to build a single-molecule detection platform, biofunctionalization should be limited to a single active site by opening a micron window on the protective layer over the SWCNT channel surface via electron beam lithography.

4.2. Single-Biomolecule Detections Based on Single-Walled Carbon Nanotube-Based Sensors

Since the first SWCNT-FETs were demonstrated in 1998,[62] a variety of SWCNT-based devices have been reported for efficient applications in numerous areas. Employing a variety of novel device configurations, fabrication techniques, and functionalization strategies, SWCNT-based field-effect biosensors have been designed to sensitively detect protein, DNA, and DNA-enzyme at the single-molecule level. In these fields of biomedical, biological, and chemical detections, it is always an important concern to improve the sensitivity of biosensors. In comparison with the doping approaches for conventional semiconductor transistors made of bulk materials, the SWCNTs as channel materials cannot simply be doped in the same way. Meanwhile, owing to the unique 1D tubular structure, the contact between SWCNTs and metal electrodes is Schottky contact, forming a narrow energy barrier of about a few nanometers. Although the energy band will be bent near the contact point between SWCNTs and electrodes due to the different work functions, the change in the electrical field of the SWCNT surface still can alter the channel current amplitude efficiently. Therefore, the SWCNTs, in which every atom on the surface is exposed to the environment, have emerged as remarkably promising electronic materials for the manufacture of highly sensitive sensor devices.

When a lysozyme molecule was tethered to a carbon nanotube field-effect sensor, the electrical signals could accurately monitor the conformational changes of proteins, uncovering the dynamic disorder (**Figure 6**a).[18] Notably, the single-molecule electrical signals from lysozyme-tethered nano-biosensors have distinct advantages, such as high bandwidth, good stability, and high temporal resolution, demonstrating the huge potential of single-molecule field-effect sensing techniques.

Over the past decade, owing to the fast conformation transition of DNA polymerase, great efforts have been made to identify and characterize the intermediate conformation trajectories in real time. Recently, a masterful strategy for the direct detection of the dynamics within single-molecule Taq DNA polymerase, using the field-effect sensor consisting of a non-covalent functionalization SWCNT was reported. Specifically, the individual Taq molecule was attracted to the channel surface of SWCNT-based sensors by a pyrene-maleimide linker (Figure 6b).[63] In the temperature-dependent catalytic experiment, the excursions of a featureless $1/f$ noise band were assigned to Taq's catalytic closures (Figure 6c). With the increase in temperature (from 45 to 72°C), the rate and duration of the transient closures and the catalytic events almost stayed constant, but the rate of the open state increased. This work demonstrates that the temperature dependence of Taq DNA polymerase catalysis depends only on the rate in the open state, which provides sufficient evidence for the evolution of high-temperature enzymes. Moreover, the point-functionalized SWCNT-based field-effect biosensor can also offer significantly high-quality transduction signals to characterize DNA hybridization kinetics (Figure 6d).[64] In the study of genomic diagnostics-based FETs, changing temperature is the common method to modulate DNA hybridization and melting. However, the repulsive electrostatic force under 300 mV gate bias can produce the same effect as temperature modulation to promote melting and inhibit hybridization (Figure 6e).

4.3. Expansion of Single-Walled Carbon Nanotube-Based Single-Molecule Biosensors

Although SWCNT-based electronic devices have been demonstrated as a powerful and reliable sensing platform associated with single-molecule detection, the practical application scope of SWCNT-based field-effect sensors has still been severely restricted by the low fabrication yield and complex fabrication process. Highly integrated and multiplexed large sensor arrays are considered as the development trend of the next-generation sensors. As shown in **Figure 7**a, an example of large single-molecule sensing arrays was fabricated on arbitrary substrates, adopting the approaches of spin-casting low densities of SWCNTs and controllable diazonium covalent functionalization.[59] To validate the sensing capabilities of the array devices, the two-point-functionalized sensor (Figure 7b, top) and the single-point-functionalized device (Figure 7b, bottom) were performed to sense DNA melting dynamics. The DNA hybridization and melting kinetics are characterized by random telegraph signals. Low and high conductance levels represented hybridized and melted lysozyme states of the probe molecule, respectively.

SWCNT-based single-molecule biosensors with a simple framework and clear sensing principle can be easily combined with other single-molecule technologies. The universal single-molecule sensing mechanism is the direct and sensitive detection of the transconductance change on the SWCNT channel. Yet, a novel idea is to build a force nano-sensor in combination with dual-trap single-molecule optical tweezers to monitor the non-covalent interaction on SWCNT sidewalls (Figure 7c).[65] Through directly measuring the binding force between a suspended SWCNT and a single DNA base, the π coupling equilibrium force was achieved about 1.2 ± 0.5 pN (Figure 7d). Furthermore, based on the above research, integrating the single-molecule force spectroscopy and field-effect electricity platform will be a new avenue to fundamentally understand the intrinsic mechanisms of the intermolecular interface at the single-molecule level.

5. 2D Materials-Based Single-Molecule Biosensors

2D materials are a new class of nanomaterials, which have sheet structures with a thickness of one or several atoms, with transverse dimensions ranging from a few nanometers to several hundred nanometers or more.[66] The superior optical, electrical, and

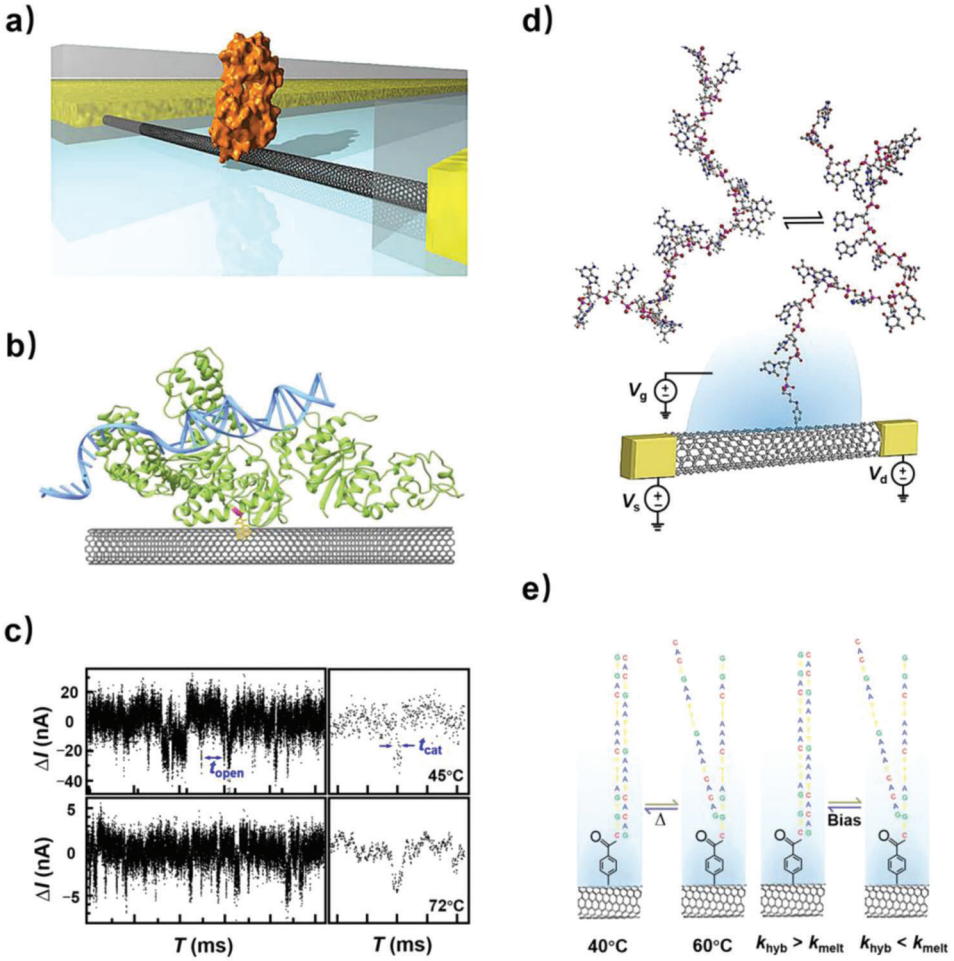

Figure 6. SWCNT-based single-molecule biosensors. a) Schematic of the single protein (lysozyme) sensing. Reproduced under terms of the CC-BY license.[18] Copyright 2012, The Authors, published by American Association for the Advancement of Science. b) Schematic of non-covalent functionalization of SWCNT-based biosensor to detect Taq DNA polymerase catalysis. c) Temperature dependence of $\Delta I(t)$ of Taq DNA polymerase. b,c) Reproduced under terms of the CC-BY-NC license.[63] Copyright 2022, The Authors, published by American Association for the Advancement of Science. d) Schematic of point-functionalized SWCNT-based biosensor to characterize DNA hybridization dynamics. e) Schematic of temperature and gate bias interfering DNA hybridization dynamics. d,e) Reproduced under terms of the CC-BY license.[64] Copyright 2017, The Authors, published by Springer Nature.

electrochemical properties of 2D materials make them promising platforms or probes for sensitive electrochemical and optical biosensors, which can be used to detect biomolecules. A large family of 2D materials has been reported, such as graphene, transition metal dichalcogenides, black phosphorene, graphitization carbonitride, hexagonal boron nitride, black arsenic phosphorene, carbonitrides, and so on. Among them, graphene, one kind of 2D nanomaterial composed of carbon atoms in a honeycomb lattice structure with atomic thickness, has attracted great interest due to its excellent optical transparency, high carrier mobility, high specific surface area, high electrical conductivity, and flexibility. Owing to these excellent properties of graphene as well as molybdenum disulfide (MoS_2) for single-molecule biosensing, we mainly take graphene and MoS_2 as examples to introduce the major development of single-molecule biosensors based on 2D materials in recent years, such as device fabrication, strategies to improve device sensitivity, and applications in the detection of single biomolecule based on 2D materials.

5.1. Fabrication of 2D Materials-Based Biosensors

The exploration and further applications of 2D materials depend on the development of fabrication methods, which can be roughly divided into bottom-up synthesis methods and top-down exfoliation methods, represented by CVD and mechanical exfoliation, respectively.

In bottom-up synthesis methods, CVD has been widely used to fabricate large-area 2D films because of the superiorities in density, high crystallinity, and uniformity.[67] In this method, the thermal decomposition of gaseous precursors on specific substrates (metals, semiconductors, or insulations) creates 2D material layers. The thickness of 2D material layers can be controlled by varying deposition parameters, such as temperature, precursor, pressure, and gas flow rate, especially the substrate.[68] For example, large area and adlayer-free monolayer graphene can be fabricated on Cu-Ni (111) alloy foils.[69] The growth of graphene on insulators and semiconductors, such as SiO_2 and sapphire, is

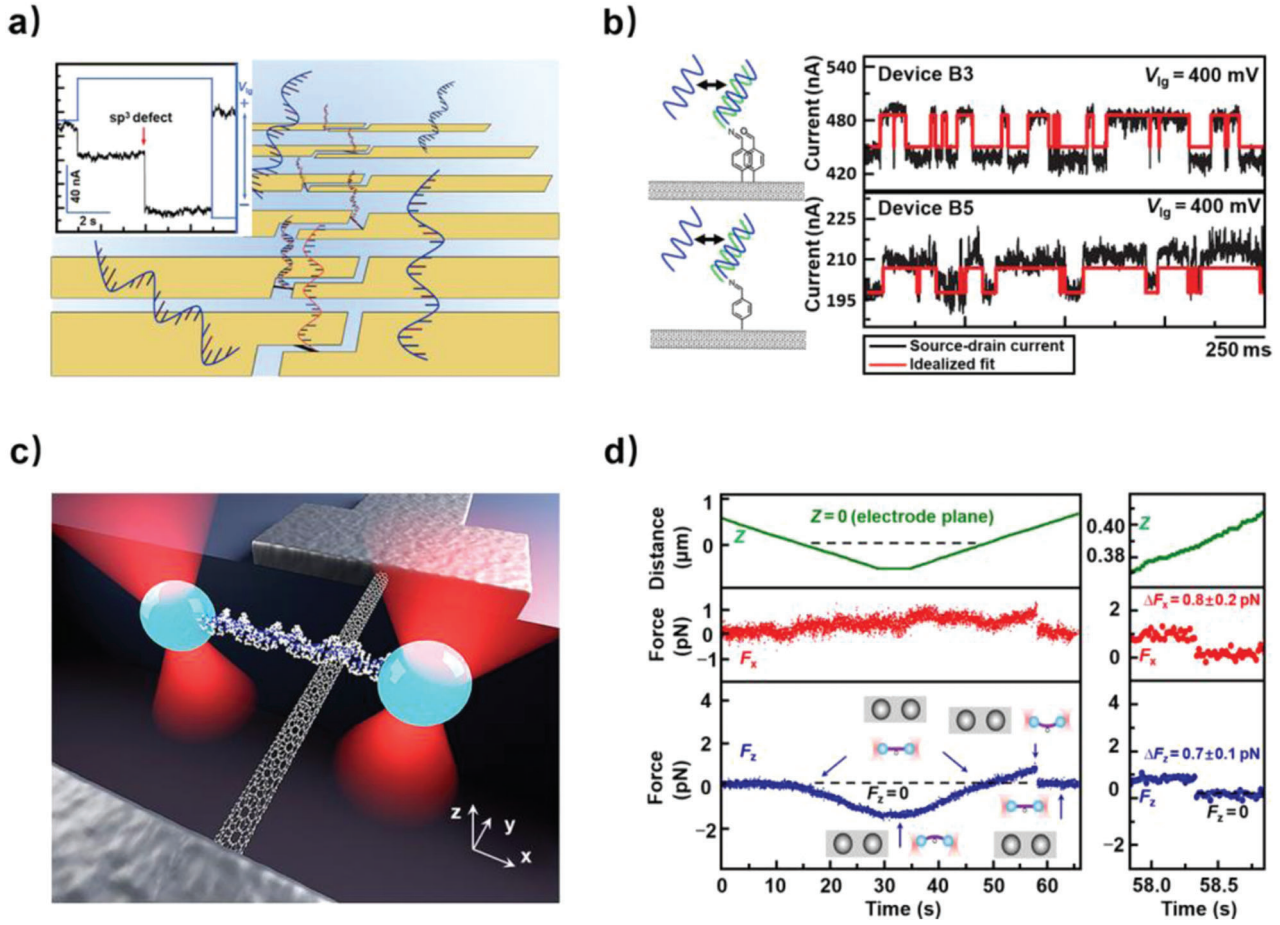

Figure 7. Expanded techniques of SWCNT-based single-molecule biosensors. a) Schematic of the SWCNT-based single-molecule sensing arrays. b) Two-level random signals for the point-functionalized SWCNT sensor. a,b) Reproduced with permission.[59] Copyright 2018, American Chemical Society. c) Schematic of the direct measurement of the π coupling force by combing the SWCNT-based biosensor with optical tweezers. d) Optical traps applied forces to control the distance between the hybrid DNA and the CNT, measuring the equilibrium force. c,d) Reproduced with permission.[65] Copyright 2018, American Chemical Society.

essential to achieve high-performance graphene devices, which prevents contamination and wrinkles introduced during the wet transfer that is used to transfer a single layer of graphene to a target substrate. In addition, plasma-enhanced CVD has been demonstrated to have a very short deposition time and a lower growth temperature (600–900°C) to avoid the high growth temperature (1000–1200°C) requirement of traditional thermal CVD.

The mechanism of the top-down method is to overcome the interlayer van der Waals interactions between bulk 2D materials with the assistance of external energy, that is, exfoliating one or several atomic layers from bulk materials.[70] A variety of methods have been developed to exfoliate 2D graphene, including scotch tape exfoliation, alkali metal intercalation-assisted exfoliation, modified mechanical exfoliation, extrinsic corrugation-assisted exfoliation, anode bonding exfoliation, and so on. According to the exfoliation mechanism, the exfoliation methods can be divided into three main types: intercalation-assisted expansion and exfoliation, exfoliation of layer materials with guest ions or molecules between the host layers, and mechanical force-assisted exfoliation.[71] In addition to the two classical methods mentioned above, a recent research has placed particular emphasis on the large-scale preparation of 2D nanomaterials such as graphene. The principle of the flash joule heating method is to convert current directly and efficiently into thermal energy as it passes through a resistor.[72] Since the resistance consists of a carbon-based starting material, it is heated to very high temperatures, leading to the cleavage of bonds and reorganization into a thermodynamically favored sp^2 hybridization of graphene sheets. This method enables large-scale production of graphene materials that weigh more than 200 mg or have a film area of more than 200 square centimeters.

Due to the inherent defects of graphene such as hydrophobicity, zero band gap, and chemical stability, it is difficult to directly apply graphene to biomolecule detection. Graphene is often processed into nanostructures, such as graphene nanoribbons (GNR), graphene nanopores, and so on. Several methods have been reported to fabricate GNR. The top-down approach includes lithography of graphene, unzipping of carbon nanotubes, and metal-assisted etching of graphene, which are conducive to the fabrication of large-area GNRs. For example, crystal GNRs can be extracted from nitrogen-doped carbon nanotubes by a two-step process of electrochemical and sonochemical treatments.[73]

With mild electrochemical unzipping, a damage-minimization unzipping can be initiated from the nitrogen doping point, followed by a longitudinal unzipping induced by sonochemical treatment in an organic solvent, and then the crystal nanoribbon structure can be fully unzipped. The bottom-up approach mainly includes solution synthesis and on-surface synthesis, which can control the edge and structure of the GNRs. For instance, hierarchical on-surface synthesis of GNR heterojunctions has been reported, which allows bottom-up growth of GNRs that preferentially display individual heterojunction interfaces rather than a random statistical sequence of junctions along the ribbon.[74] The strategy for achieving this hierarchical growth relies on functionalizing the first GNR precursor with iodine and the second GNR precursor with bromine. The linking element is the second precursor of GNR, which is replaced by iodine on one side and bromine on the other. Such heterojunctions provide a viable platform that can be used directly at the molecular scale for GNR-based functional device applications.

To further improve the performance of 2D materials-based single-molecule sensors, single nanoscale holes, as small as single-atomic vacancies, can be introduced into atomically thin 2D films to generate nanopores devices. In general, 2D nanopores can be formed by etching holes in an existing substrate and then fabricating nanoribbons on the modified substrate or transferring nanoribbons to this substrate. For instance, hybrid plasma nanopores were fabricated by directly depositing a single flake of MoS_2 on metallic holes without the use of complex lithographic processes.[75] The device is implemented on silicon nitride membranes and can be further refined by transmission electron microscopy or focused ion beam milling to allow a molecule to pass through nanopores. This strategy can be applied not only to MoS_2, but also to many other 2D materials, where the defects in the layers can be used to anchor the linkers between metal nanopores and sheets.

5.2. Single-Molecule Sensitivity of 2D Material-Based Biosensors

It is necessary to improve the sensitivity of sensors based on 2D materials to realize their detection at the single-molecule level. In general, the sensitivity of devices can be improved by processing 2D materials into nanoribbons or nanopores to match the single-molecule size.

GNRs are lengthened 1D, monolayer strips of graphene with a hexagonal honeycomb lattice structure. GNR has the advantages of high conductivity, ultrahigh surface area, high adsorption, fast response, high sensitivity, and selectivity, which make it an emerging biosensing platform. The unique structure of GNRs makes them more sensitive than other graphene-based materials in single-molecule detection. For instance, an amino acid nanosensor can be constructed based on a single-armchair GNR.[76] The electrical properties of the sensors before and after the adsorption of different amino acids on armchair GNRs were calculated. The results showed that the density of the projected state and the transmission function, *T*, changed significantly during the adsorption process with a distinct response to specific amino acids.

Due to the resistance reduction of 2D nanopores, when molecules pass through 2D nanopores, thin nanopores will generate large ion currents, and only a small part of molecules or even a single molecule stays in the pore channel in a given time, which is conducive to accurate detection of a single molecule. For instance, a hybrid plasma 2D material structure has been proposed to generate a significant field confinement near nanopores.[75] The plasma enhancement provided by nanopores is strongly accumulated in 2D nanopores, thus representing an ideal system for single-molecule sensing and sequencing in flow configurations.

In addition to the above two strategies, MoS_2-based sensors are more sensitive in detecting biomolecules, which surpass the sensitivity of that based on graphene by more than 74-fold.[77] The lower density of interface states at the semiconductor-dielectric interface of MoS_2 not only allows for better control of static electricity, but also reduces low-frequency noises, one of the main sources of noises for FET biosensors. Therefore, in comparison with graphene-based biosensors, MoS_2-based FET biosensors have a higher field-effect switching ratio and higher molecular detection response. It has been shown that both MoS_2 nanopores and MoS_2 surfaces can be used for single DNA base detection. The band gap of MoS_2 changes significantly when the bases are placed above the original MoS_2 and the tailored MoS_2 nanoribbon, making MoS_2 a promising material for base detection through transverse current tunneling measurements.

5.3. Single-Biomolecule Detections on 2D Material-Based Biosensors

2D materials are favored in the field of DNA detection because of their good biocompatibility, high signal intensity, and biological binding sites. To further achieve ultra-high sensitivity, label-free DNA detection at the single-molecule level, two different detection methods have been confirmed, one is the fabrication of nanopores in the nanoribbon and the other is the side-wall detection based on the nanoribbon. Here, we mainly summarize the latest application progress of single-molecule biosensing based on 2D materials in DNA detection from the above two aspects.

When a single DNA molecule passes through the nanopore at an applied potential, the nucleotide sequence can be ideally read by monitoring small changes in the ionic current flowing through the pore caused by a single nucleotide temporarily residing within the nanopore. Particularly, the nanopores matching the molecular size of the nanoribbons limit the area through which the molecules can pass, making it easier to achieve single-molecule detection. Therefore, ultra-thin films such as graphene and monolayers of MoS_2 may provide greater sensitivity for nanopore DNA sequencing. For instance, the integration of a solid-state SiN_x nanopore with a GNR transistor can create a DNA translocation sensor (**Figure 8**a).[78] It has been shown that non-electrostatic base-specific interactions between DNA bases and GNRs lead to changes in local state density around the nanopore, resulting in changes in the resistivity of the nanoribbons, which can be measured by in-plane currents passing through the nanoribbons.[79] As shown in Figure 8b, when DNA molecules pass through the nanopore, the device can simultaneously measure the drops in ionic current and changes in local voltage in the transistor, both of which can be used to detect the molecule. On the whole, the use of 2D materials such

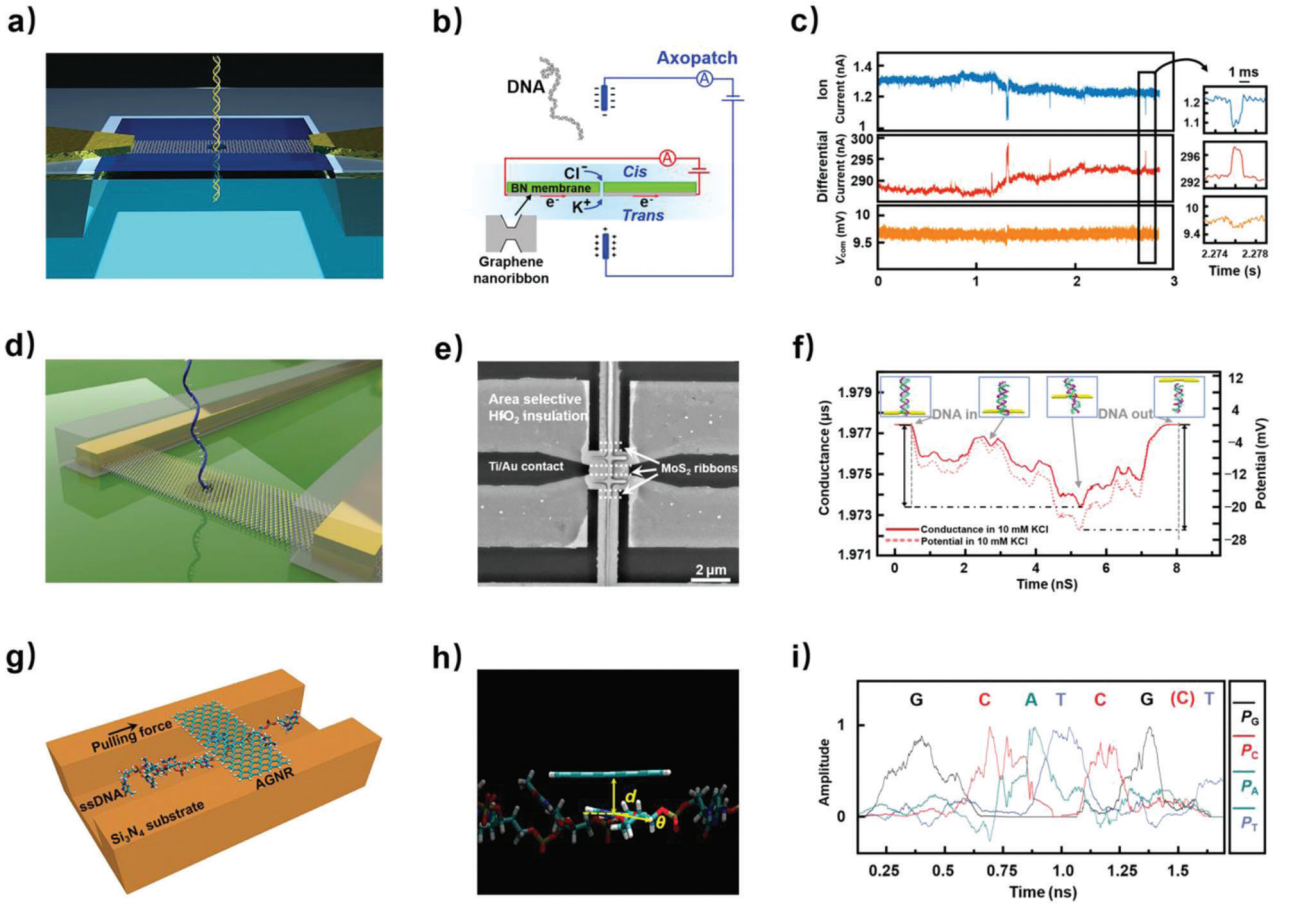

Figure 8. Single-molecule DNA detections by 2D material-based biosensors. a) Schematic representation of the GNR transistor–nanopore device. Reproduced with permission.[78] Copyright 2013, Macmillan Publishers Limited. b) Schematic of the graphene nanoribbon-nanopore measuring setup. c) During the translocation of DNA through the nanopore, the ion current and the graphene current change synchronously. b,c) Reproduced with permission.[79] Copyright 2018, American Chemical Society. d) Schematic of a MoS_2 FET-nanopore device. e) TEM image of the MoS_2 FET-nanopore device. d,e) Reproduced with permission.[81] Copyright 2019, American Chemical Society. f) Potential and transverse conductance change synchronously as the translocation of DNA through the MoS_2 nanopore. Reproduced with permission.[80] Copyright 2020, American Chemical Society. g) Schematic of a nanochannel device with an armchair GNR for ssDNA passing. h) A simulated instantaneous snapshot of DNA passing through GNR channels. i) Simulation signals achieve the resolution of individual bases. g–i) Reproduced with permission.[85] Copyright 2011, Macmillan Publishers Limited.

as GNRs has the potential added value, as it allows the detection of DNA translocation through two simultaneous signals: A plane current through the nanoribbon and an ion current through the nanopore (Figure 8c).

In comparison with graphene nanopores, MoS_2 has a strong field effect and is less likely to clog nanopores with DNA. A systematic microscopic analysis of various electrical resistance effects involved in the electrical detection of a single biomolecule in MoS_2 nanoribbons shows that there is a self-consistent interaction between ions, carriers around the pore rim, and biomolecules.[80] The sensitivity of the MoS_2 nanopore biosensor can be improved by amplifying the value of electron conductance variation (Figure 8f), which captures the characteristics of the DNA translocation signal. Therefore, MoS_2 has been widely used in DNA sequencing. An electrically contacted MoS_2 nanoribbon integrated with a nanopore has been proposed. Using field-effect sensing, DNA molecules are sensed by the associated signals of ionic currents passing through the nanopore and transverse currents passing through the nanoribbon (Figure 8d), the charge of the molecule is directly sensed by the nanoribbon.[81] As shown in Figure 8e, three ribbons are fabricated on each membrane, only one of which has an independent part (suspended over the aperture of the SiN_x membrane). In order to solve the problem of fast translocation of DNA through nanopore membranes, a viscosity gradient system based on room-temperature ionic liquids was proposed to control the translocation dynamics of DNA through the MoS_2 nanopore.[82] The physical and chemical properties of room-temperature ionic liquids can be tailored to a given application. When DNA is translocated in the pore, the non-translocated part of the DNA polymer-monomers will retain the coil conformation and be subject to the strong Stokes dragging force of the ionic liquid. As a result, DNA translocation through the pore can be significantly slowed. Therefore, the technology that utilizes the high viscosity of room-temperature ionic liquids can be used for statistical detection of all four types of nucleotides and provide optimal single nucleotide translocation speeds for DNA sequencing while maintaining a SNR above 10.

In addition, some novel and reliable works have been carried out to improve the sensitivity and efficiency of nanopore-nanoribbon DNA detection. For instance, a design of a biomolecular detection platform based on large-scale parallel solid-state nanopores has been proposed via simulations.[83] The double-pore system is modeled as a parallel resistance circuit. It is shown that the transverse sheets' current along the membrane is not affected by the crosstalk effect of biomolecules translocating through multiple pores simultaneously because they can only sense the change of local potential. Electronic sensing across nanopore membranes provides higher detection resolution compared to ionic current blocking techniques in a multipore setup, regardless of the irregularities that occur when a nanopore is manufactured in a 2D membrane. Also, large-area manufacturing of MoS_2 nanopore devices by wafer-scale growth, fabrication, and transfer of MoS_2 films has been demonstrated. The method has the potential to create nanopores simultaneously in situ by electrically isolating each device from the other, making it a scalable method for producing individual nanopores on the same wafer.[84]

The side-wall response of limiting the passage of a single molecule through nanoribbon can be used as the basis of single-molecule detection (Figure 8g). The feasibility of using a fluidic nanochannel functionalized with a GNR for DNA sequencing (Figure 8h) has been theoretically demonstrated to overcome some issues of DNA passing through the nanopore in the nanoribbon, such as controlling the DNA translocation rate, suppressing stochastic nucleobase motions, and resolving the signal overlap between different nucleobases (Figure 8i).[85] The approach involves deciphering the changes in the conductance of nanoribbons as a result of their interactions with the nucleobases via π–π stacking. Experimental implementation of this device promises ultra-fast and reliable DNA sequencing.

6. Molecular-Bridge-Based Single-Molecule Biosensors

In addition to SiNWs, SWCNTs, and 2D materials, molecular bridges can also connect source and drain electrodes to realize single-molecule electrical detection. According to the function of biomolecules, molecular-bridge-based biosensors can be divided into two main categories: biomolecules acting as probe molecules on the side of organic molecular bridges (such as organic conductive polymers) and biomolecules themselves acting as the molecular bridge (usually DNA and proteins). The molecular bridges for building single-molecule biosensors have some similar characteristics. First of all, molecules selected as charge transport materials are generally conductive with simple and precise structures. Second, they should have suitable terminal groups for self-assembling between the nano-gapped electrodes. In addition, if the biomolecules behave as a probe, the conductive polymer should have a site-specific conjugation part for attaching probe biomolecules.

6.1. Single-Biomolecule Sensing Based on Organic Molecular Bridges

In the first category, polymers with high conductivity can be used as molecular bridges.[13] For example, the protein α-helices are mainly used as molecular wires for the detection of molecular interactions. In order to selectively bind and self-assemble the protein to metal nanoelectrodes, the electrode-specific terminal groups are required at the ends of the α-helix.[86] The self-assembly process is usually based on dielectrophoresis due to the shorter time it takes, instead of passive diffusion where ions or small molecules with high concentrations are transported to low-concentration parts of the solution driven by the concentration difference or potential difference.[87] If the bridged molecule is non-polarizable, the whole self-assembly will consume 24 h. However, a polarizable molecule (such as α-helix) can decrease the required time. During the dielectrophoresis process, the polarizable bridged molecules are attracted to the nanoelectrodes by electrical forces under a fixed asymmetric electric field, and therefore the assembly is greatly enhanced and accelerated. The whole process can be completed in 10 s. To only detect one probe molecule at a time, there should be only one specific conjugation site in the middle of the α-helix, which is the attachment site for probe molecules. Then, a certain probe molecule that can interact with target molecules is selected to be conjugated with the molecular bridge to realize specific detection of target molecules.

There are many kinds of probe molecules, such as DNA oligos, aptamers, antibodies, antigens, and some enzymes. Single-stranded DNA (ssDNA) is a typical probe molecule. A 14 monomeric unit (14-mer) oligonucleotide, which can interact with ssDNA, is added around the molecular bridge in a particular concentration.[13] When the binding between the probe ssDNA and the target 14-mer oligo is formed, the baseline current change can be detected at the same time (**Figure 9**a). Similarly, utilizing the ssDNA as a probe molecule, the interaction between antigen and antibody can be detected. Specifically, the antifluorescein antibody can be detected on the electronic biosensor via interaction with the ssDNA oligo. The oligo is designed with the fluorescein antigen at its 3'(distal) end (Figure 9b).

Meanwhile, aptamers as a special kind of oligonucleotides can also interact with proteins for single-biomolecule sensing. The main advantage of those aptamers is that they can interact with various target substances while maintaining high specificity and selectivity, so they are widely used in the field of biosensors.[88–90] Furthermore, some special proteins can also be used as probe molecules. Take deoxy-ribonucleoside triphosphate (dNTP) (the protein) and polymerase (the small molecule) as an example. This kind of biosensor usually tethers a DNA template to the bridge and then binds a complementary primer oligo to the structure. The complementary primer further formed a probe site as a polymerase-binding probe. As shown in Figure 9c, the DNA polymerase enzyme can also be conjugated to the molecular bridge by a site-specific conjugation method. Therefore, single-molecule electronic biosensors with conductive polymer bridges have powerful functions and great potential for practical applications in biomedical sciences.

6.2. Single-Biomolecule Sensing Based on Nucleic Acid Molecular Transport

In addition to polymer-based sensing bridges, biomolecules themselves can also be directly connected to the nanoelectrodes to build single-molecule electronic devices for studying

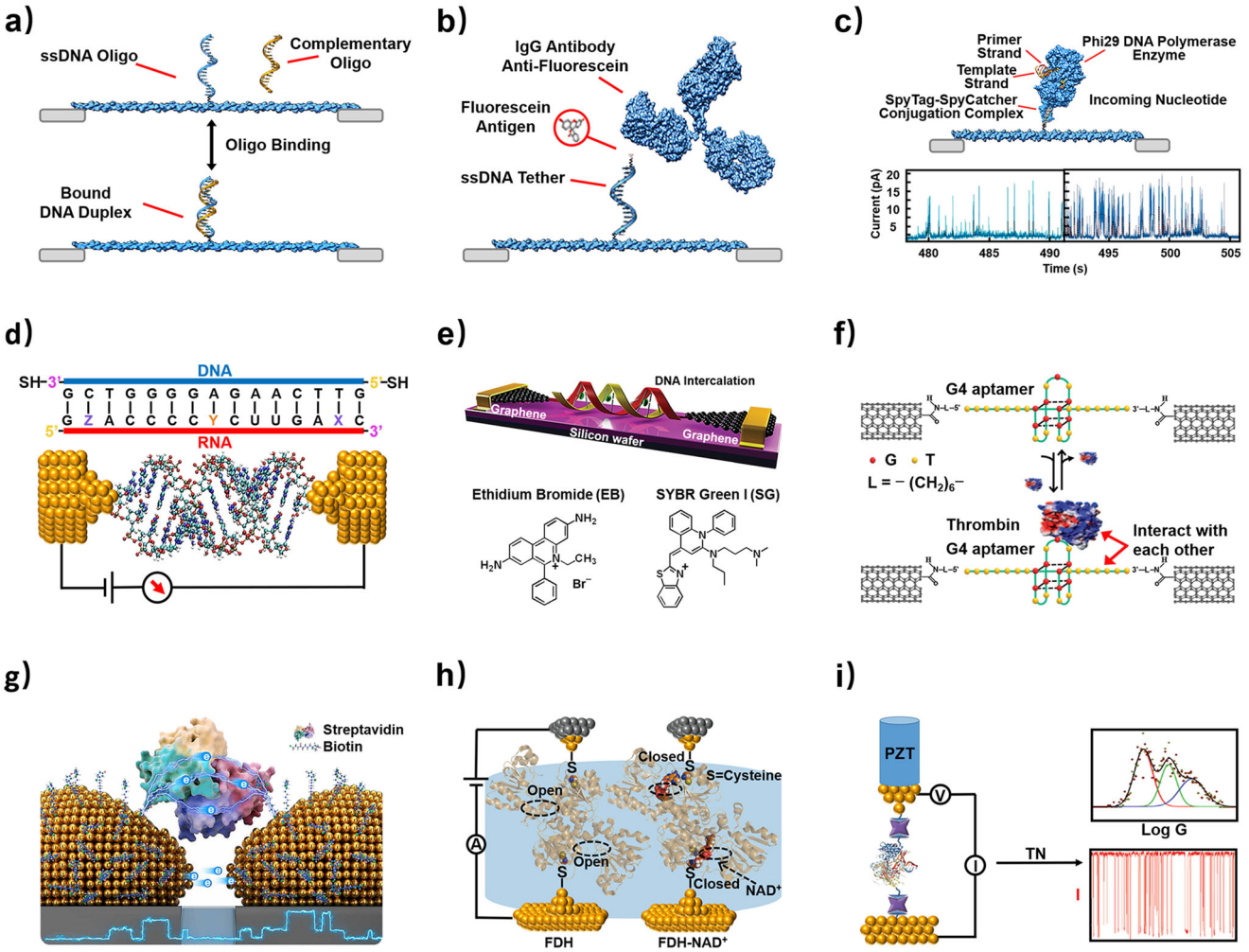

Figure 9. Molecular-bridge-based single-molecule biosensors. a) Schematic of the ssDNA oligo probe and polymer biosensor. b) Schematic of the antibody-antigen polymer biosensor. c) Schematic of the DNA polymerase activity polymer biosensor. a–c) Reproduced under terms of the CC-BY-NC-ND license.[13] Copyright 2022, The Authors, published by National Academy of Science. d) RNA/DNA hybrid in single-molecule junction for single-base detection. Reproduced with permission.[96] Copyright 2018, Springer Nature. e) Schematic representation of a DNA-functionalized molecular junction and the structures of EB and SG. Reproduced with permission.[99] Copyright 2015, The Royal Society of Chemistry. f) Schematic representation of the G4 aptamer junction and the binding process between the aptamer and the thrombin for the detection of the conductance. Reproduced with permission.[105] Copyright 2011, Wiley-VCH. g) Schematic representation of the stand-alone QMT probe which was functionalized with thiolated biotin and used to capture individual streptavidin molecules. Reproduced under terms of the CC-BY license.[107] Copyright 2022, The Authors, published by Association for the Advancement of Science. h) Schematic of the single-molecule FDH and FDH-NAD^+ junctions. Reproduced under terms of the CC-BY-NC-ND license.[111] Copyright 2020, The Authors, published by Elsevier. i) Schematic representation of the capture of the Φ29 polymerases by SA trapped by electrodes. The right-hand-side panels show the conductance changes of the polymerases (top) and rapid fluctuations in current when a nonspecific contact activated (bottom). Reproduced with permission.[113] Copyright 2019, American Chemical Society.

biological properties. Due to the superior sequence-specific self-assembly properties and density of functionalities embedded in its framework, DNA can be used in the development of functional nanoscale devices and materials.[91] The possibility of charge transport (CT) over significant distances of the stacked aromatic base pairs and the conductive properties of duplex DNAs will contribute to DNA as a sensing molecular element.[92]

It is found that DNA can be used as a molecular bridge to connect the SWCNT electrodes. The DNA of interest is coupled to the SWCNT electrodes through amide linkages.[93] However, single-base mismatches may dramatically attenuate mediate CT in a variety of experiments. The DNA duplexes and mismatches are further explored, and it is found that the mismatched devices have higher resistance than corresponding devices with well-matched DNA. Meanwhile, replacing the mismatched complement with the original well-matched sequence can recover the original on-state resistance and nanoamp current levels. These demonstrate the sensitivity of DNA CT to perturbations in stacking and suggest that DNA may not be appropriate to serve as a robust wire for nanoelectronic circuits. Therefore, DNA molecules bridging nanodevices can surely transduce biochemical events into electrical signals at the single-molecule level and serve as uniquely powerful reporters.[94] In addition to the single-base detection of single DNA duplex, the CT properties of RNA/DNA hybrids are

also sensitive to single-nucleotide polymorphisms and the sensitivity mainly arises from the effects of mutations of the molecular conformational structure, thereby realizing single-base detection. Furthermore, RNA can also be used to extract biologically relevant information from short RNA oligonucleotides through single-molecule conductance techniques and this can be used to detect target molecules of interest.[95] For example, athogenic bacterial strains from the transcribed RNA sequences of the strains were directly detected and identified via measuring conductance changes. The RNA/DNA hybrids were injected into the electrodes and bound between two gold electrodes (Figure 9d). The conductance for four RNA/DNA hybrids, including one perfectly matched RNA sequence and the other three mismatched, was then detected and the results show that the RNA/DNA hybrids are highly sensitive to small variations in the sequence, even single-base mismatches.[96]

Moreover, when the nucleic acid is used as the molecular bridge, the interaction between DNA molecules and their environments (such as external ions, molecules, proteins, and so on) can also be sensitively detected.[97] A platform with femtomolar sensitivity and high selectivity to detect paramagnetic Cu^{2+} has been described in previous researches. The method integrates a Cu^{2+}-dependent DNAzyme into graphene-molecule junctions. By the interaction between Cu^{2+} and the DNAzyme, the direct electrical detection of paramagnetic Cu^{2+} can be realized.[98] Further studies have shown that individual molecule intercalations can also affect DNA CT.[99] Ethidium bromide (EB) is a widely used intercalator and can be used to probe the effect on the electrical properties of DNAs by the interactions between them and DNAs. The intercalations can lead to profound changes in the DNA structural integrity, and the degree of such changes depends on the intercalators.[100] The structural integrity of DNA is distorted and the distortion of DNA duplexes will reduce the DNA CT after the treatment of the EB (Figure 9e).[101] In another study, a graphene-molecule-graphene single-molecule junction (GMG-SMJ) is built to detect single-molecule cocaine-aptamer interaction.[13] The GMG-SMJ is formed by connecting the DNA strand to the nanogapped graphene electrode arrays, which are constructed with the method of dash-line lithographic.[102] To form a molecular bridge, the complementary strand, which contains the cocaine aptamer, is linked to the DNA strand through hydrogen bonds. The cocaine binding site is located in the center of the three stems of the aptamer, which has a special structure to provide a positive driving force for binding,[103] while the introduction of cocaine can change the structure of the aptamer. Since the kinetics of the cocaine conformational change is affected by an applied voltage, the GMG-SMJ is used to detect the voltage-dependent properties to clarify the effects on the structure of cocaine. Current oscillations before and after cocaine treatment have been distinctly recorded, representing real-time cocaine-aptamer interactions. This result and further concentration-dependent experiments reveal that once the aptamer is binding with cocaine, distinct current oscillations can be detected, demonstrating the dynamic mechanism of the conformational changes of the aptamer.

The interaction between DNA and protein can also be detected in carbon nanotube devices except for interacting with ions and molecules. As one kind of single-stranded nucleic acid ligand, aptamers can function primarily in molecular recognition and have advantages in the detection of target proteins compared with antibodies. Therefore, the 15-mer thrombin aptamer with thymine 7 linkers on both the 3' and 5' termini (Apt-A) assumes a G-quadruplex (G4) conformation when it binds with the target human thrombin with a high binding affinity (Figure 9f), which is more suitable for real-time selective detection of thrombin than an antibody. The formation of G4 conformation is an important feature of Apt-A and this structure can be significantly stabilized by metal ions (K^+ or Mg^{2+}) to keep a high binding affinity.[104] On this basis, when the Atp-A interacts with the thrombin and the conductance changes are reversible, a sharp increase in conductance can be detected.[105]

6.3. Single-Biomolecule Sensing Based on Protein Molecular Transport

In addition to DNA molecules, proteins can also act as molecular bridges because of their excellent characteristics such as self-assembly into highly repeatable complexes, and extensive molecular recognition capabilities.[106] So far, studies have shown that proteins themselves are capable of sensing as the molecular bridge. For example, a large amount of consensus tetratricopeptide repeat proteins were synthesized, whose lengths are from 4 to 20 nm with an increment of 4 nm, respectively. Their different conductance properties can be explored via scanning tunneling microscopy (STM) measurements, showing the current in the experiment decays slowly with increasing the length. Based on the experiment results and the analysis of the transport mechanism of proteins in a long transport range, the potential of proteins as molecular bridges is proved.

Furthermore, the conformational properties of proteins are distinguished by studying the transport properties of molecular bridges. For instance, by fabricating quantum mechanical tunneling probes (Figure 9g), the biotin-streptavidin-biotin junction was formed successfully and then the conductance properties under a wide range of bias voltages were obtained via two nnaogapped nanoelectrodes in a stand-alone double-barrel nanopipette. The four conductance states indicate the different conformations of proteins. The protein conformational change under the electric field may influence bias-dependent stochastic switching characteristics in the transport process, thus influencing the conductance. This is a great contribution to the study of conformational states related to biological processes.[107] By using wild-type streptavidin as a connector in bioelectronic circuits and connecting a doubly biotinylated polymerase to electrodes, the electrode surface potential can be modified by charged residues at the protein contact points, which can strongly regulate the overall conductance, providing more possibilities for proteins to act as molecular bridges.[108]

The protein-based molecular bridge can also help to study the reaction, function of the protein, and interaction with other materials. For instance, formate dehydrogenase (FDH), an important oxidoreductase as a coenzyme among the bioactive proteins, can form carbon dioxide through the electric coupling with nicotinamide adenine dinucleotide (NAD^+).[109] By donating electrons from FDH to NAD^+, the process of the oxidation of the formate to CO_2 is realized. However, owing to the technical challenges in the characterization of CT through bioactive

enzymes, the relationship between CT through coenzymes and their bioactivities is unclear. To solve the problem, the STM break junction (STM-BJ) is used to capture the CT through single active FDH systems to investigate the coupling between the FDH and NAD^+. STM-BJ, which is capable of forming thousands of single-molecule junctions repeatedly, has rapidly been used in conductance-structure correlation studies to reveal the effect of intramolecular and intermolecular interactions through single-molecule conductance.[110] To detect the conductance during the interaction between FDH and NAD^+, the active FDH is immobilized between the substrate and gold tip covered with an apiezon wax via forming the Au-S bond from the L-cysteines. During the breaking process, by applying a constant bias potential between two gold electrodes, adding NAD^+ into the solution around the electrodes, and moving the gold tip upward from the substrate, the conductance changes, and a molecule conductance plateau forms (Figure 9h). After adding NAD^+ and nicotinamide adenine dinucleotide phosphate which is seen as a coenzyme into the solution, the conductance of NAD^+ shows a significant increase. This suggests that the coupling between FDH and coenzymes may boost the CT process.[111]

However, if the proteins are directly connected to electrodes, the extent of research to detect ligand binding changes or the accompanying conformation change is limited because the active sites are tied up by the fixed electrical contact point. By taking advantage of the redox inactive nature of the proteins, proteins can also conduct well if they are in contact with the binding agents which can inject charge carriers into their interiors.[112] This allows a single protein molecule to be wired into an electrical sensing circuit acting as enzymes and be used as sensors, detectors, or sequencing devices. The protein with specially designed contact points can bind to functionalized electrodes with binding agents, which can further increase the conductance. The streptavidin molecule which can use two of the four binding sites as contact points is captured by electrodes functionalized with thiolated biotin to study the change of conductance as additional biotin molecules bind (Figure 9i).[113]

7. Photoelectric System for Single-Molecule Sensing

As discussed above, the electrical detection platforms based on nanoscale circuits are particularly attractive because of their remarkable advantages such as real-time measurement, high-time resolution, and integration capability.[10] With the development of single-molecule optical technology, optical imaging detection has been widely used due to its unique advantages, including non-contact, high sensitivity, high precision, and 2D image metrology. Based on both single-molecule electrical detection and optical detection, a new and promising technique of photoelectric integration is proposed, which can combine the characteristics of both two detection technologies. The enhanced sensitivity of the integrated system can not only reveal the electronic properties of target biomolecules, but also report their precise sensing sites and optical properties. Therefore, simultaneous optical and electrical detection provides a new opportunity to better understand the single molecule dynamics activity.

Among all optical detection methods, fluorescence is one of the most efficient single-molecule detection methods due to its high sensitivity and selectivity. The single-molecule fluorescence technology refers to reaching a nano-scale resolution of single-molecule imaging and detection via detecting the emitted fluorescence from the fluorescent groups under the excitation of light with a specific wavelength. Since the emitted fluorescence of single molecules is weak, unique fluorescence detection methods are required, for example, fluorescence correlation spectroscopy (FCS),[114] fluorescence recovery after photobleaching,[115] photo-induced electron transfer,[116] and fluorescence resonance energy transfer (FRET),[117] which has been widely used by its high level of generality. In FRET, when the emission spectrum of the donor fluorescent molecule overlaps with the absorption spectrum of the acceptor fluorescent molecule, and the distance between two molecules is within 10 nm, energy is typically transferred between donor and acceptor molecules. After the energy transfer process, donor fluorescence is extinguished and acceptor fluorescence is enhanced significantly. Therefore, by labeling two different fluorescent groups on a biological molecule or two interacting molecules, the distance between the two molecules can be determined. Meanwhile, the conformational changes of biological molecules with time in life activities can be predicted by FRET.[118]

In addition, detection techniques are also important for molecular scale imaging. The fluorescent microscopy technology mainly includes two categories. One is traditional far-field microscopy, which contains total internal reflection fluorescence (TIRF), confocal laser scanning microscope, etc. The other is super-resolution microscopy which has been awarded the 2014's Nobel Prize in Chemistry for its ability to break the original optical diffraction limit and achieve nano-scale resolution. Super-resolution microscopy mainly includes stimulated emission depletion (STED),[119] photo-activated light microscopy (PALM),[120] STORM,[121] and fluorescence-PALM.[122] STED shows high spatial resolution by only detecting emitted fluorescence in the non-overlapping region of two lasers while that of the surrounding molecules is not detected. It is the first far-field microscopy that breaks the diffraction limit. The other three kinds achieve super-resolution by making only a very small fraction of the fluorophores emit light at a time, and accumulating this process multiple times to obtain the whole image.[123]

The development of single-molecule fluorescence detection techniques provides a foundation for the detection of single biomolecules, particularly for the study of single bio-dynamics. For instance, the dynamics of DNA transcription can be studied via single-molecule fluorescence imaging. The composition and catalytic status of the initial Escherichia coli transcription-coupled repair (TCR) mechanism can be characterized in real time. By labeling fluorescent components (RNA polymerase, mutation frequency decline, or RNA) to the complex, the composition and localization of the complex can be monitored through the TIRF imaging system, showing the whole TCR process.[124] In addition to the study of DNA dynamics, the dynamics of other biomolecules, such as proteins, can also be detected. For example, by improving the FCS method, a new single-molecule 2D fluorescence lifetime correlation spectrum method is applied to quantitatively clarify the microsecond conformational dynamics of proteins. In this method, a 2D emission-delay correlation map of single molecules is obtained and then converted to the fluorescence lifetime. The different fluorescence lifetimes of

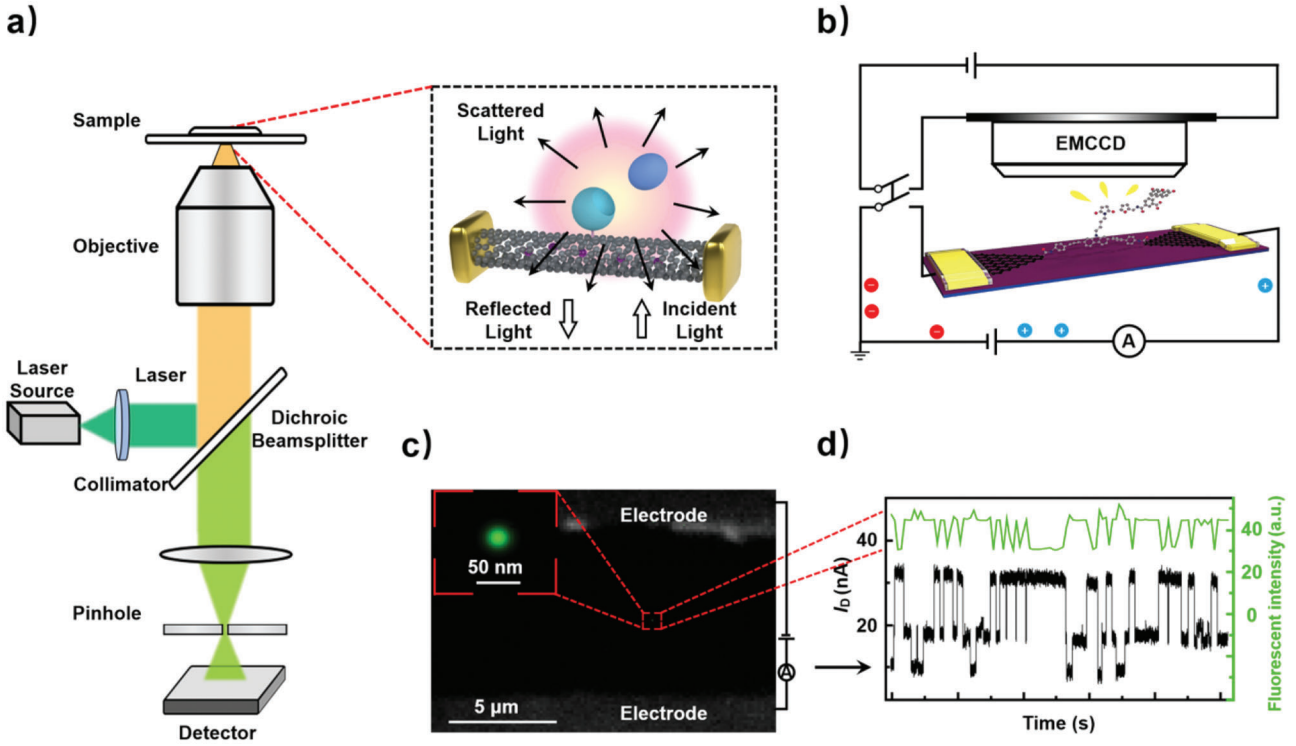

Figure 10. Photoelectric single-molecule sensing system. a) A fluorescence microscopic imaging device, including excitation laser and illumination path, with an enlarged sample stand. It can be seen that the laser emits incident light, the reflected light passes through the pinhole and gathers on the APD, and the sample also emits scattered light. b) Schematic of the synchronous sensing system of optical and electrical signals, where optical signals are obtained through electron-multiplying charge-coupled device (EMCCD). c) A super-resolution fluorescence microscope image of a single-molecule connection. d) Current and fluorescent signals are monitored synchronously during the reaction. b–d) Reproduced under terms of the CC-BY-NC license.[126] Copyright 2021, The Authors, Association for the Advancement of Science.

FRET donors can reveal different protein structures at the single molecule level, showing the complex conformational dynamics of proteins at a wide range of time scales.[125]

With the rapid development of single-molecule detection technology, the combination of electrical and optical detection of single molecules has gradually been applied to the study of single-molecule biodynamics, especially on the single molecular junction. By analyzing the interference of light generated via rayleigh scattering and reflection of the incident laser beam, the unmarked detection and super-resolution imaging with nanometer positioning accuracy can be realized (**Figure 10**a). For instance, the GMG-SMJ is formed to observe the dynamics of single-molecule Diels-Alder reaction by forming covalent bonds between the molecular bridge with amino terminals and the graphene electrodes. The successful connection of single molecules and the reaction position of the catalyst can be demonstrated by the external super-resolution microscopic imaging system (Figure 10b). By combining optical detection and electrical detection, the fluorescence intensity and electrical signal can be detected synchronously. As shown in Figure 10c,d, the two signals match well when the bridged single molecule undergoes the Diels-Alder reaction. The highest conductance corresponds to quenching fluorescence, the lowest conductance corresponds to the highest fluorescence intensity, and the intermediate conductance corresponds to relatively weak quenching), indicating that the bridged molecule is the reaction center.[126]

Similar to the above experiment, other works are also carried out in the way of photoelectric combinations. By covalently integrating a single-molecule Pd catalyst into the nano-notched graphene point electrodes, a stable GMG-SMJ is fabricated to explain the mechanism of Suzuki-Miyaura cross-coupling. After forming a single-molecule junction, determining that only one catalyst molecule is connected between the two electrodes through single-molecule resolution fluorescence imaging. By comparing the fluorescence signal and current signal of a single-molecule catalyst in real-time, the change in fluorescence intensity is completely consistent with the electrical signal, which strongly proves the successful fabrication of a single-molecule junction.[127]

To sum up, the fluorescence technique is a powerful complement to assist with capturing radiant photons from a biomolecule of interest, for obtaining a deeper understanding of the single-molecule behavior. The combination of optical and electrical detection technologies has been effectively realized in single-molecule junctions, which can provide both electrical and optical characteristics of single-biomolecule sensing.

8. Conclusion

Single-molecule electronic biosensors, which reach the final limit of analytic chemistry, are one of the most exciting technologies toward single-molecule detection for life science and biomedical

applications in the past decade. This review has systematically summarized the prominent advances related to single-molecule electronic biosensors, with a particular focus on alternative sensing configurations based on four specific channel materials, including SiNWs, SWCNTs, 2D nanomaterials, and molecular bridges. In this field, a lot of amazing advances have been made, such as label-free, highly sensitive, and high-bandwidth detection at the single-molecule level. In particular, some methods can fabricate arrays of biosensors on arbitrary substrates. However, for further commercial applications, single-molecule electronic sensing techniques still face some challenges, such as reducing electronic noise, scalable fabrication, and system integration.

So far, most single-molecule electronic biosensors are carried out in ideal media, and biological samples need to be pretreated to reduce the impact of environmental noises, which greatly hinders practical applications. The output current signals based on single-molecule electronic biosensors are usually at the order of nA and in the kHz bandwidth, which means that the input-referred root mean square noise should be controlled below hundreds of pA. Efficient integrated packaging design on the electronic biosensors is an effective way to enhance device stability and alleviate this problem. What's more, IC miniaturization and integration with the electronic readout circuits are other promising strategies. It can not only decrease noise by reducing stray and interconnection capacitances, but also permit the implementation of multi-biomarker detection on one chip. Arranging individual readout biosensors into a compact and efficient array is also an inevitable requirement for building highly integrated and multiplexed biosensor architectures.

In addition, with the continuous development of single-molecule detection techniques, the optical and electrical cooperative system is also a promising method, which can provide additional optical information to single-molecule electronic biosensors. Single-molecule optical and spectroscopic methods, such as single-molecule Raman spectroscopy, single-molecule fluorescence, super-resolution imaging, and near-field optics, also provide a powerful toolbox. The combination of single-molecule optical and electrical techniques provides more detailed and accurate information for the in-depth study of single-biomolecule behaviors. In future studies, these collaboration modes and optimization strategies still require a lot of efforts to determine the system framework more suitable for single-molecule biosensors, which deserves intensive researches.

Acknowledgements

The authors acknowledge primary financial supports from the National Key R&D Program of China (2021YFA1200102, 2021YFA1200101, and 2022YFE0128700), the National Natural Science Foundation of China (22150013, 22173050, 21727806, and 21933001), the Fundamental Research Funds for the Central Universities (63223056), the Tencent Foundation through the XPLORER PRIZE, "Frontiers Science Center for New Organic Matter" at Nankai University (63181206), the Natural Science Foundation of Beijing (2222009), and Beijing National Laboratory for Molecular Sciences (BNLMS202105).

Conflict of Interest

The authors declare no conflict of interest.

Keywords

biosensors, field effect, fluorescence, low dimensional materials, single molecule

Received: November 29, 2022
Revised: January 17, 2023
Published online: February 2, 2023

[1] D. Xiang, X. Wang, C. Jia, T. Lee, X. Guo, *Chem. Rev.* **2016**, *116*, 4318.
[2] P. Li, C. Jia, X. Guo, *Chem. Rec.* **2021**, *21*, 1284.
[3] S. Sorgenfrei, C. Y. Chiu, R. L. Gonzalez Jr., Y. J. Yu, P. Kim, C. Nuckolls, K. L. Shepard, *Nat. Nanotechnol.* **2011**, *6*, 126.
[4] E. Macchia, K. Manoli, B. Holzer, C. Di Franco, M. Ghittorelli, F. Torricelli, D. Alberga, G. F. Mangiatordi, G. Palazzo, G. Scamarcio, L. Torsi, *Nat. Commun.* **2018**, *9*, 3223.
[5] Y. Li, C. Yang, X. Guo, *Acc. Chem. Res.* **2020**, *53*, 159.
[6] Y. Wang, J. Irudayaraj, *Philos. Trans. R. Soc., B* **2013**, *368*, 20120026.
[7] X. Lu, P. R. Nicovich, K. Gaus, J. J. Gooding, *Biosens. Bioelectron.* **2017**, *93*, 1.
[8] R. V. Ovali, R. Sahin, A. Bek, M. E. Tasgin, *Appl. Phys. Lett.* **2021**, *118*, 241103.
[9] K. C. Neuman, A. Nagy, *Nat. Methods* **2008**, *5*, 491.
[10] C. Gu, C. Jia, X. Guo, *Small Methods* **2017**, *1*, 1700071.
[11] S. Mao, J. Chang, H. Pu, G. Lu, Q. He, H. Zhang, J. Chen, *Chem. Soc. Rev.* **2017**, *46*, 6872.
[12] X. Guo, *Adv. Mater.* **2013**, *25*, 3397.
[13] C. W. Fuller, P. S. Padayatti, H. Abderrahim, L. Adamiak, N. Alagar, N. Ananthapadmanabhan, J. Baek, S. Chinni, C. Choi, K. J. Delaney, R. Dubielzig, J. Frkanec, C. Garcia, C. Gardner, D. Gebhardt, T. Geiser, Z. Gutierrez, D. A. Hall, A. P. Hodges, G. Hou, S. Jain, T. Jones, R. Lobaton, Z. Majzik, A. Marte, P. Mohan, P. Mola II, P. Mudondo, J. Mullinix, T. Nguyen, et al., *Proc. Natl. Acad. Sci. USA* **2022**, *119*, e2112812119.
[14] A. K. Wanekaya, W. Chen, N. V. Myung, A. Mulchandani, *Electroanalysis* **2006**, *18*, 533.
[15] F. Yang, G.-J. Zhang, *Rev. Anal. Chem.* **2014**, *33*, 95.
[16] J. Zou, Q. Zhang, *Adv. Sci.* **2021**, *8*, 2102860.
[17] Q. Hu, S. Chen, P. Solomon, Z. Zhang, *Sci. Adv.* **2021**, *7*, eabj6711.
[18] Y. Choi, I. S. Moody, P. C. Sims, S. R. Hunt, B. L. Corso, I. Perez, G. A. Weiss, P. G. Collins, *Science* **2012**, *335*, 319.
[19] W. M. Parkin, M. Drndic, *ACS Sens.* **2018**, *3*, 313.
[20] W. Fu, L. Jiang, E. P. van Geest, L. M. Lima, G. F. Schneider, *Adv. Mater.* **2017**, *29*, 1603610.
[21] R. Elnathan, M. Kwiat, A. Pevzner, Y. Engel, L. Burstein, A. Khatchtourints, A. Lichtenstein, R. Kantaev, F. Patolsky, *Nano Lett.* **2012**, *12*, 5245.
[22] S. Sorgenfrei, C. Y. Chiu, M. Johnston, C. Nuckolls, K. L. Shepard, *Nano Lett.* **2011**, *11*, 3739.
[23] Z. Zheng, H. Zhang, T. Zhai, F. Xia, *Chin. J. Chem.* **2021**, *39*, 999.
[24] K. Maehashi, T. Katsura, K. Kerman, Y. Takamura, K. Matsumoto, E. Tamiya, *Anal. Chem.* **2007**, *79*, 782.
[25] R. J. Chen, H. C. Choi, S. Bangsaruntip, E. Yenilmez, X. Tang, Q. Wang, Y.-L. Chang, H. Dai, *J. Am. Chem. Soc.* **2004**, *126*, 1563.
[26] S. Mukherjee, X. Meshik, M. Choi, S. Farid, D. Datta, Y. Lan, S. Poduri, K. Sarkar, U. Baterdene, C. E. Huang, Y. Y. Wang, P. Burke, M. Dutta, M. A. Stroscio, *IEEE Trans. Nanobiosci.* **2015**, *14*, 967.
[27] N. Nakatsuka, K.-A. Yang, J. M. Abendroth, K. M. Cheung, X. Xu, H. Yang, C. Zhao, B. Zhu, Y. S. Rim, Y. Yang, *Science* **2018**, *362*, 319.
[28] N. Gao, W. Zhou, X. Jiang, G. Hong, T.-M. Fu, C. M. Lieber, *Nano Lett.* **2015**, *15*, 2143.
[29] Q. Li, N. Lu, L. Wang, C. Fan, *Small Methods* **2018**, *2*, 1700263.

[30] L. Baraban, B. Ibarlucea, E. Baek, G. Cuniberti, *Adv. Sci.* **2019**, *6*, 1900522.
[31] D. Yin, J. Li, J. Feng, W. Liu, Z. Yang, S. Li, M. Li, L. Li, X. Guo, *J. Mater. Chem. C* **2022**, *10*, 469.
[32] C. Jia, Z. Lin, Y. Huang, X. Duan, *Chem. Rev.* **2019**, *119*, 9074.
[33] J. Wang, F. Shen, Z. Wang, G. He, J. Qin, N. Cheng, M. Yao, L. Li, X. Guo, *Angew. Chem., Int. Ed.* **2014**, *53*, 5038.
[34] M. Sarpras, R. Gaur, V. Sharma, S. S. Chhapekar, J. Das, A. Kumar, S. K. Yadava, M. Nitin, V. Brahma, S. K. Abraham, N. Ramchiary, *PLoS One* **2016**, *11*, e0167791.
[35] X. Yang, A. Gao, Y. Wang, T. Li, *Nano Res.* **2018**, *11*, 1520.
[36] J. Ma, M. Du, C. Wang, X. Xie, H. Wang, T. Li, S. Chen, L. Zhang, S. Mao, X. Zhou, M. Wu, *ACS Sens.* **2021**, *6*, 3367.
[37] H. Zhang, N. Kikuchi, N. Ohshima, T. Kajisa, T. Sakata, T. Izumi, H. Sone, *ACS Appl. Mater. Interfaces* **2020**, *12*, 51808.
[38] L. Syedmoradi, A. Ahmadi, M. L. Norton, K. Omidfar, *Mikrochim Acta* **2019**, *186*, 739.
[39] J. Li, Y. Zhang, S. To, L. You, Y. Sun, *ACS Nano* **2011**, *5*, 6661.
[40] G. Yuan, Y. Zhou, C. Guo, W. Zhang, Y. Tang, Y. Li, Z. Chen, Z. He, X. Zhang, P. Wang, *ACS Nano* **2010**, *4*, 3045.
[41] Z. Yang, C. Qi, W. Liu, D. Yin, L. Yu, L. Li, X. Guo, *J. Phys. Chem. Lett.* **2021**, *12*, 3853.
[42] A. I. Efimova, E. A. Lipkova, K. A. Gonchar, D. E. Presnov, A. A. Eliseev, A. V. Pavlikov, V. Y. Timoshenko, *J. Raman Spectrosc.* **2020**, *51*, 2146.
[43] H. Peretz-Soroka, A. Pevzner, G. Davidi, V. Naddaka, R. Tirosh, E. Flaxer, F. Patolsky, *Nano Lett.* **2013**, *13*, 3157.
[44] P. Xie, Q. Xiong, Y. Fang, Q. Qing, C. M. Lieber, *Nat. Nanotechnol.* **2011**, *7*, 119.
[45] A. Gao, X. Yang, J. Tong, L. Zhou, Y. Wang, J. Zhao, H. Mao, T. Li, *Biosens. Bioelectron.* **2017**, *91*, 482.
[46] J. Li, G. He, U. Hiroshi, W. Liu, H. Noji, C. Qi, X. Guo, *ACS Nano* **2017**, *11*, 12789.
[47] W. P. Hu, C. C. Tsai, Y. S. Yang, H. W. Chan, W. Y. Chen, *Sci. Rep.* **2018**, *8*, 12598.
[48] W. C. Chou, W. P. Hu, Y. S. Yang, H. W. Chan, W. Y. Chen, *Sci. Rep.* **2019**, *9*, 11056.
[49] G. He, J. Li, H. Ci, C. Qi, X. Guo, *Angew. Chem., Int. Ed.* **2016**, *55*, 9036.
[50] G. He, J. Li, C. Qi, X. Guo, *Adv. Sci.* **2017**, *4*, 1700158.
[51] W. Liu, J. Li, Y. Xu, D. Yin, X. Zhu, H. Fu, X. Su, X. Guo, *Adv. Sci.* **2021**, *8*, 2101383.
[52] S. Alwarappan, A. Erdem, C. Liu, C.-Z. Li, *J. Phys. Chem. C* **2009**, *113*, 8853.
[53] B. L. Allen, P. D. Kichambare, A. Star, *Adv. Mater.* **2007**, *19*, 1439.
[54] B. Cai, Y. Su, Z. Tao, J. Hu, C. Zou, Z. Yang, Y. Zhang, *Adv. Opt. Mater.* **2018**, *6*, 1800791.
[55] N. Yang, X. Chen, T. Ren, P. Zhang, D. Yang, *Sens. Actuators, B* **2015**, *207*, 690.
[56] J. Prasek, J. Drbohlavova, J. Chomoucka, J. Hubalek, O. Jasek, V. Adam, R. Kizek, *J. Mater. Chem. A* **2011**, *21*, 15872.
[57] O. T. Gul, K. M. Pugliese, Y. Choi, P. C. Sims, D. Pan, A. J. Rajapakse, G. A. Weiss, P. G. Collins, *Biosensors* **2016**, *6*, 29.
[58] D. Bouilly, J. Hon, N. S. Daly, S. Trocchia, S. Vernick, J. Yu, S. Warren, Y. Wu, R. L. Gonzalez Jr., K. L. Shepard, C. Nuckolls, *Nano Lett.* **2016**, *16*, 4679.
[59] Y. Lee, S. M. Trocchia, S. B. Warren, E. F. Young, S. Vernick, K. L. Shepard, *ACS Nano* **2018**, *12*, 9922.
[60] T. J. Olsen, Y. Choi, P. C. Sims, O. T. Gul, B. L. Corso, C. Dong, W. A. Brown, P. G. Collins, G. A. Weiss, *J. Am. Chem. Soc.* **2013**, *135*, 7855.
[61] K. M. Pugliese, O. T. Gul, Y. Choi, T. J. Olsen, P. C. Sims, P. G. Collins, G. A. Weiss, *J. Am. Chem. Soc.* **2015**, *137*, 9587.
[62] S. J. Tans, M. H. Devoret, R. J. Groeneveld, C. Dekker, *Nature* **1998**, *394*, 761.
[63] M. W. Turvey, K. N. Gabriel, W. Lee, J. J. Taulbee, J. K. Kim, S. Chen, C. J. Lau, R. E. Kattan, J. T. Pham, S. Majumdar, *Sci. Adv.* **2022**, *8*, eabl3522.
[64] S. Vernick, S. M. Trocchia, S. B. Warren, E. F. Young, D. Bouilly, R. L. Gonzalez, C. Nuckolls, K. L. Shepard, *Nat. Commun.* **2017**, *8*, 15450.
[65] T. Hong, T. Wang, Y.-Q. Xu, *Nano Lett.* **2018**, *18*, 7883.
[66] N. Rohaizad, C. C. Mayorga-Martinez, M. Fojtu, N. M. Latiff, M. Pumera, *Chem. Soc. Rev.* **2021**, *50*, 619.
[67] W. Liu, M. Liu, X. Liu, X. Wang, H. X. Deng, M. Lei, Z. Wei, Z. Wei, *Adv. Opt. Mater.* **2020**, *8*, 1901631.
[68] R. Kumar, S. Sahoo, E. Joanni, R. K. Singh, R. M. Yadav, R. K. Verma, D. P. Singh, W. K. Tan, A. P. del Pino, S. A. Moshkalev, A. Matsuda, *Nano Res.* **2019**, *12*, 2655.
[69] M. Huang, M. Biswal, H. J. Park, S. Jin, D. Qu, S. Hong, Z. Zhu, L. Qiu, D. Luo, X. Liu, Z. Yang, Z. Liu, Y. Huang, H. Lim, W. J. Yoo, F. Ding, Y. Wang, Z. Lee, R. S. Ruoff, *ACS Nano* **2018**, *12*, 6117.
[70] J. Li, X. Liu, Y. Feng, J. Yin, *Prog. Polym. Sci.* **2022**, *126*, 101505.
[71] X. Cai, Y. Luo, B. Liu, H. M. Cheng, *Chem. Soc. Rev.* **2018**, *47*, 6224.
[72] K. M. Wyss, D. X. Luong, J. M. Tour, *Adv. Mater.* **2022**, *34*, 2106970.
[73] H. J. Lee, J. Lim, S. Y. Cho, H. Kim, C. Lee, G. Y. Lee, S. P. Sasikala, T. Yun, D. S. Choi, M. S. Jeong, H. T. Jung, S. Hong, S. O. Kim, *ACS Appl. Mater. Interfaces* **2019**, *11*, 38006.
[74] C. Bronner, R. A. Durr, D. J. Rizzo, Y.-L. Lee, T. Marangoni, A. M. Kalaylian, H. Rodriguez, W. Zhao, S. G. Louie, F. R. Fischer, M. F. Crommie, *ACS Nano* **2018**, *12*, 2193.
[75] D. Garoli, D. Mosconi, E. Miele, N. Maccaferri, M. Ardini, G. Giovannini, M. Dipalo, S. Agnoli, F. De Angelis, *Nanoscale* **2018**, *10*, 17105.
[76] S. Bagherzadeh-Nobari, R. Kalantarinejad, S. M. Elahi, S. Sanvito, *Sens. Actuators, B* **2018**, *255*, 1276.
[77] D. Sarkar, W. Liu, X. Xie, A. C. Anselmo, S. Mitragotri, K. Banerjee, *ACS Nano* **2014**, *8*, 3992.
[78] F. Traversi, C. Raillon, S. M. Benameur, K. Liu, S. Khlybov, M. Tosun, D. Krasnozhon, A. Kis, A. Radenovic, *Nat. Nanotechnol.* **2013**, *8*, 939.
[79] S. J. Heerema, L. Vicarelli, S. Pud, R. N. Schouten, H. W. Zandbergen, C. Dekker, *ACS Nano* **2018**, *12*, 2623.
[80] M. Xiong, M. Graf, N. Athreya, A. Radenovic, J. P. Leburton, *ACS Nano* **2020**, *14*, 16131.
[81] M. Graf, M. Lihter, D. Altus, S. Marion, A. Radenovic, *Nano Lett.* **2019**, *19*, 9075.
[82] J. Feng, K. Liu, R. D. Bulushev, S. Khlybov, D. Dumcenco, A. Kis, A. Radenovic, *Nat. Nanotechnol.* **2015**, *10*, 1070.
[83] N. B. M. Athreya, A. Sarathy, J. P. Leburton, *ACS Sens.* **2018**, *3*, 1032.
[84] M. Thakur, M. Macha, A. Chernev, M. Graf, M. Lihter, J. Deen, M. Tripathi, A. Kis, A. Radenovic, *Small Methods* **2020**, *4*, 2000072.
[85] S. K. Min, W. Y. Kim, Y. Cho, K. S. Kim, *Nat. Nanotechnol.* **2011**, *6*, 162.
[86] U. O. Seker, H. V. Demir, *Molecules* **2011**, *16*, 1426.
[87] R. Zhuravel, H. Huang, G. Polycarpou, S. Polydorides, P. Motamarri, L. Katrivas, D. Rotem, J. Sperling, L. A. Zotti, A. B. Kotlyar, J. C. Cuevas, V. Gavini, S. S. Skourtis, D. Porath, *Nat. Nanotechnol.* **2020**, *15*, 836.
[88] Z. Chen, Q. Wu, J. Chen, X. Ni, J. Dai, *Virol Sin* **2020**, *35*, 351.
[89] Y. Song, J. Song, X. Wei, M. Huang, M. Sun, L. Zhu, B. Lin, H. Shen, Z. Zhu, C. Yang, *Anal. Chem.* **2020**, *92*, 9895.
[90] N. K. Singh, P. Ray, A. F. Carlin, C. Magallanes, S. C. Morgan, L. C. Laurent, E. S. Aronoff-Spencer, D. A. Hall, *Biosens. Bioelectron.* **2021**, *180*, 113111.
[91] F. A. Aldaye, A. L. Palmer, H. F. Sleiman, *Science* **2008**, *321*, 1795.
[92] S. Delaney, J. K. Barton, *J. Org. Chem.* **2003**, *68*, 6475.
[93] X. Guo, J. P. Small, J. E. Klare, Y. Wang, M. S. Purewal, I. W. Tam, B. H. Hong, R. Caldwell, L. Huang, S. O'brien, *Science* **2006**, *311*, 356.
[94] X. Guo, A. A. Gorodetsky, J. Hone, J. K. Barton, C. Nuckolls, *Nat. Nanotechnol.* **2008**, *3*, 163.

[95] L. Venkataraman, J. E. Klare, C. Nuckolls, M. S. Hybertsen, M. L. Steigerwald, *Nature* **2006**, *442*, 904.
[96] Y. Li, J. M. Artes, B. Demir, S. Gokce, H. M. Mohammad, M. Alangari, M. P. Anantram, E. E. Oren, J. Hihath, *Nat. Nanotechnol.* **2018**, *13*, 1167.
[97] X. Xie, W. Xu, X. Liu, *Acc. Chem. Res.* **2012**, *45*, 1511.
[98] L. Gao, L. L. Li, X. Wang, P. Wu, Y. Cao, B. Liang, X. Li, Y. Lin, Y. Lu, X. Guo, *Chem. Sci.* **2015**, *6*, 2469.
[99] X. Wang, L. Gao, B. Liang, X. Li, X. Guo, *J. Mater. Chem. B* **2015**, *3*, 5150.
[100] I. D. Vladescu, M. J. McCauley, M. E. Nunez, I. Rouzina, M. C. Williams, *Nat. Methods* **2007**, *4*, 517.
[101] J. C. Genereux, J. K. Barton, *Chem. Rev.* **2010**, *110*, 1642.
[102] Y. Cao, S. Dong, S. Liu, L. He, L. Gan, X. Yu, M. L. Steigerwald, X. Wu, Z. Liu, X. Guo, *Angew. Chem., Int. Ed.* **2012**, *51*, 12228.
[103] M. N. Stojanovic, D. W. Landry, *J. Am. Chem. Soc.* **2002**, *124*, 9678.
[104] E. Baldrich, A. Restrepo, C. K. O'Sullivan, *Anal. Chem.* **2004**, *76*, 7053.
[105] S. Liu, X. Zhang, W. Luo, Z. Wang, X. Guo, M. L. Steigerwald, X. Fang, *Angew. Chem., Int. Ed.* **2011**, *50*, 2496.
[106] B. Zhang, E. Ryan, X. Wang, W. Song, S. Lindsay, *ACS Nano* **2022**, *16*, 1671.
[107] L. Tang, L. Yi, T. Jiang, R. Ren, B. Paulose Nadappuram, B. Zhang, J. Wu, X. Liu, S. Lindsay, J. B. Edel, *Sci. Adv.* **2022**, *8*, eabm8149.
[108] B. Zhang, E. Ryan, X. Wang, S. Lindsay, *J. Am. Chem. Soc.* **2021**, *143*, 15139.
[109] A. Hirose, T. Kasai, M. Aoki, T. Umemura, K. Watanabe, A. Kouzuma, *Nat. Commun.* **2018**, *9*, 1083.
[110] R. Sha, L. Xiang, C. Liu, A. Balaeff, Y. Zhang, P. Zhang, Y. Li, D. N. Beratan, N. Tao, N. C. Seeman, *Nat. Nanotechnol.* **2018**, *13*, 316.
[111] X. Zhuang, A. Zhang, S. Qiu, C. Tang, S. Zhao, H. Li, Y. Zhang, Y. Wang, B. Wang, B. Fang, W. Hong, *iScience* **2020**, *23*, 101001.
[112] B. Zhang, S. Lindsay, *Nano Lett.* **2019**, *19*, 4017.
[113] B. Zhang, H. Deng, S. Mukherjee, W. Song, X. Wang, S. Lindsay, *ACS Nano* **2020**, *14*, 1360.
[114] J. J. La Clair, *J. Am. Chem. Soc.* **1997**, *119*, 7676.
[115] E. A. Reits, J. J. Neefjes, *Nat. Cell Biol.* **2001**, *3*, E145.
[116] S. Doose, H. Neuweiler, M. Sauer, *ChemPhysChem* **2009**, *10*, 1389.
[117] T. Ha, *Methods* **2001**, *25*, 78.
[118] S. Deindl, W. L. Hwang, S. K. Hota, T. R. Blosser, P. Prasad, B. Bartholomew, X. Zhuang, *Cell* **2013**, *152*, 442.
[119] T. A. Klar, S. W. Hell, *Opt. Lett.* **1999**, *24*, 954.
[120] E. Betzig, G. H. Patterson, R. Sougrat, O. W. Lindwasser, S. Olenych, J. S. Bonifacino, M. W. Davidson, J. Lippincott-Schwartz, H. F. Hess, *Science* **2006**, *313*, 1642.
[121] M. J. Rust, M. Bates, X. Zhuang, *Nat. Methods* **2006**, *3*, 793.
[122] S. T. Hess, T. P. Girirajan, M. D. Mason, *Biophys. J.* **2006**, *91*, 4258.
[123] T. Chen, B. Dong, K. Chen, F. Zhao, X. Cheng, C. Ma, S. Lee, P. Zhang, S. H. Kang, J. W. Ha, W. Xu, N. Fang, *Chem. Rev.* **2017**, *117*, 7510.
[124] E. T. Graves, C. Duboc, J. Fan, F. Stransky, M. Leroux-Coyau, T. R. Strick, *Nat. Struct. Mol. Biol.* **2015**, *22*, 452.
[125] T. Otosu, K. Ishii, T. Tahara, *Nat. Commun.* **2015**, *6*, 7685.
[126] C. Yang, Z. Liu, Y. Li, S. Zhou, C. Lu, Y. Guo, M. Ramirez, Q. Zhang, Y. Li, Z. Liu, *Sci. Adv.* **2021**, *7*, eabf0689.
[127] C. Yang, L. Zhang, C. Lu, S. Zhou, X. Li, Y. Li, Y. Yang, Y. Li, Z. Liu, J. Yang, K. N. Houk, F. Mo, X. Guo, *Nat. Nanotechnol.* **2021**, *16*, 1214.

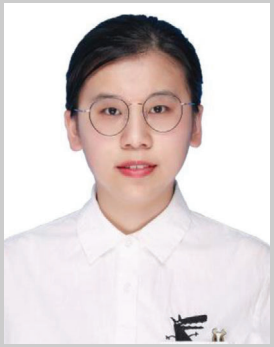

Xinyue Chang is currently a Ph.D. candidate in the Center of Single-Molecule Sciences, Institute of Modern Optics, College of Electronic Information and Optical Engineering, Nankai University, with Prof. Xuefeng Guo. Her research is focused on single-molecule devices and dynamics.

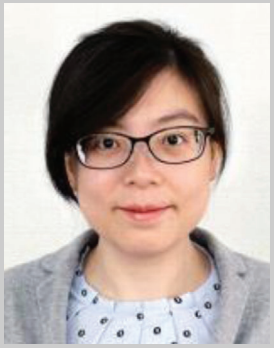

Jinying Wang received her B.S. degree in 2009 from Beijing Normal University and her Ph.D. degree in 2014 from the College of Chemistry and Molecular Engineering, Peking University, Beijing. From 2015 to 2017, she was a Post-Doctor at the University of Tokyo, Japan. Then, she worked as a Post-Doctor at Purdue University till now. Her current research is focused on nano-electronics and spintronics.

Chuancheng Jia received his Ph.D. degree in 2014 from the College of Chemistry and Molecular Engineering, Peking University, with Prof. Xuefeng Guo. From 2014 to 2020, he was a Postdoc at the Institute of Chemistry, Chinese Academy of Sciences, and University of California, Los Angeles. He joined the faculty as a Professor at Nankai University in 2020. His research is focused on single-molecule devices and dynamics.

Xuefeng Guo received his B.S. degree in 1998 from Beijing Normal University and his Ph.D. degree in 2004 from the Institute of Chemistry, Chinese Academy of Sciences, Beijing. From 2004 to 2007, he was a Postdoc at the Columbia University Nanocenter. He joined the faculty as a Professor under the 'Peking 100-Talent' Program at Peking University in 2008. His current research is focused on single-molecule science and technology.